# STRESSES AND DEFORMATIONS IN INVOLUTE SPUR GEARS BY FINITE ELEMENT METHOD

A Thesis Submitted to the

College of Graduate Studies and Research

in Partial Fulfillment of the Requirements

for the Degree of Master of Science

in the

Department of Mechanical Engineering

University of Saskatchewan

Saskatoon, Saskatchewan

By

Zeping Wei

# PERMISSION TO USE

In presenting this thesis in partial fulfillment of the requirements for a postgraduate degree from the University of Saskatchewan, I agree that the Libraries of the University of Saskatchewan may make this thesis freely available for inspection. I also agree that permission for extensive copying of this thesis, in whole or in part, for scholarly purposes may be granted by the professor or professors who supervised this thesis work or, in their absence, by the Head of the Department or the Dean of the College in which my thesis work was done. It is understood that due recognition shall be given to the author of this thesis and to the University of Saskatchewan in any use of the material in this thesis. Copying or publication or any other use of this thesis for financial gain without approval by the University of Saskatchewan and the author's written permission is prohibited.

Request for permission to copy or to make any other use of the material in this thesis in whole or part should be addressed to:

Head of the Department of Mechanical Engineering

57 Campus Drive

University of Saskatchewan

Saskatoon, Saskatchewan

S7N 5A9, Canada

# ACKNOWLEDGEMENTS

The author is indebted to Dr. Glen Watson and hereby would like to express her sincere appreciation and gratitude to him for his valuable guidance, help and encouragement during the process of this research work and in the preparation of this thesis. Without his guidance and support this work would have been impossible.

The author also would like to offer her sincere gratitude to Dr. Szyszkowski for his invaluable technical guidance and advice throughout the course of this research.

The author is grateful to the faculty and the staff of the Department of Mechanical Engineering, University of Saskatchewan, who have provided the most cooperative assistance to her for this research work.

The author also acknowledges the financial assistance provided by Dr. Glen Watson and the Department of Mechanical Engineering, University of Saskatchewan for a scholarship during my master studies.

The author wishes to extend her thanks to her husband Yong Zhang and her daughter Yun Zhang, who were a constant and active source of support throughout the endeavor.

# ABSTRACT

This thesis investigates the characteristics of an involute gear system including contact stresses, bending stresses, and the transmission errors of gears in mesh. Gearing is one of the most critical components in mechanical power transmission systems. Transmission error is considered to be one of the main contributors to noise and vibration in a gear set. Transmission error measurement has become popular as an area of research on gears and is possible method for quality control. To estimate transmission error in a gear system, the characteristics of involute spur gears were analyzed by using the finite element method. The contact stresses were examined using 2-D FEM models. The bending stresses in the tooth root were examined using a 3-D FEM model.

Current methods of calculating gear contact stresses use Hertz's equations, which were originally derived for contact between two cylinders. To enable the investigation of contact problems with FEM, the stiffness relationship between the two contact areas is usually established through a spring placed between the two contacting areas. This can be achieved by inserting a contact element placed in between the two areas where contact occurs. The results of the two dimensional FEM analyses from ANSYS are presented. These stresses were compared with the theoretical values. Both results agree very well. This indicates that the FEM model is accurate.

This thesis also considers the variations of the whole gear body stiffness arising from the gear body rotation due to bending deflection, shearing displacement and contact deformation. Many different positions within the meshing cycle were investigated.

# TABLE OF CONTENTS

# LIST OF FIGURES

# LIST OF TABLES

# Nomenclature

| | |
|---|---|
| $K$ | Structural stiffness |
| $u$ | Displacement vector |
| $F$ | Applied load vector |
| $P_{\max}$ | Maximum contact stress |
| $d_1$ | Pinion pitch diameter |
| $d_2$ | Gear pitch diameter |
| $F_i$ | Load per unit width |
| $R_i$ | Radius of cylinder $i$ |
| $\varphi$ | Pressure angle |
| $\upsilon_i$ | Poisson's ratio for cylinder $i$ |
| $E_i$ | Young's modulus for cylinder $i$ |
| $\sigma_H$ | Maximum Hertz stress. |
| a | Contact width |
| $r$ | Any radius to involute curve |
| $r_b$ | Radius of base circle |
| $\theta$ | Vectorial angle at the pitch circle |
| $\xi$ | Vectorial angle at the top of tooth |
| $\phi$ | Pressure angle at the pitch circle |

$\phi_1$ Pressure angle at radius $r$

$B_P^B$ Tooth displacement vectors caused by bending and shearing of the pinion

$B_g^B$ Tooth displacement vectors caused by bending and shearing of the gear

$H_P^B$ Contact deformation vectors of tooth pair B for the pinion

$H_g^B$ Contact deformation vectors of tooth pair B for the gear

$\theta_P^B$ Transverse plane angular rotation of the pinion body

$\theta_g^B$ Transverse plane angular rotation of the gear body

$p_d$ Diametral pitch

$Y$ Lewis form factor

$K_a$ Application factor

$K_s$ Size factor

$K_m$ Load distribution factor

$K_v$ Dynamic factor

$F_t$ Normal tangential load

$Y_j$ Geometry factor

$\theta_g$ Angular rotation of the output gear

$\theta_p$ Angular rotation of the input gear

# Chapter 1 INTRODUCTION

## 1.1 Research Overview

Gearing is one of the most critical components in a mechanical power transmission system, and in most industrial rotating machinery. It is possible that gears will predominate as the most effective means of transmitting power in future machines due to their high degree of reliability and compactness. In addition, the rapid shift in the industry from heavy industries such as shipbuilding to industries such as automobile manufacture and office automation tools will necessitate a refined application of gear technology.

A gearbox as usually used in the transmission system is also called a speed reducer, gear head, gear reducer etc., which consists of a set of gears, shafts and bearings that are factory mounted in an enclosed lubricated housing. Speed reducers are available in a broad range of sizes, capacities and speed ratios. Their job is to convert the input provided by a prime mover (usually an electric motor) into an output with lower speed and correspondingly higher torque. In this thesis, analysis of the characteristics of involute spur gears in a gearbox was studied using nonlinear FEM.

The increasing demand for quiet power transmission in machines, vehicles, elevators and generators, has created a growing demand for a more precise analysis of the characteristics of gear systems. In the automobile industry, the largest manufacturer of gears, higher reliability and lighter weight gears are necessary as lighter automobiles continue to be in demand. In addition, the success in engine noise reduction promotes the production of quieter gear pairs for further noise reduction. Noise reduction in gear pairs is especially critical in the rapidly growing field of office-automation equipment as the office environment is adversely affected by noise, and machines are playing an ever-

widening role in that environment. Ultimately, the only effective way to achieve gear noise reduction is to reduce the vibration associated with them. The reduction of noise through vibration control can only be achieved through research efforts by specialists in the field. However, a shortage of these specialists exists in the newer, lightweight industries in Japan [42] mainly because fewer young people are specializing in gear technology today and traditionally the specialists employed in heavy industries tend to stay where they are.

Designing highly loaded spur gears for power transmission systems that are both strong and quiet requires analysis methods that can easily be implemented and also provide information on contact and bending stresses, along with transmission errors. The finite element method is capable of providing this information, but the time needed to create such a model is large. In order to reduce the modeling time, a preprocessor method that creates the geometry needed for a finite element analysis may be used, such as that provided by Pro/Engineer. Pro/Engineer can generate models of three-dimensional gears easily. In Pro/E, the geometry is saved as a file and then it can be transferred from Pro/E to ANSYS. In ANSYS, one can click File > Import > IGES > and check No defeaturing and Merge coincident key points.

The prime source of vibration and noise in a gear system is the transmission error between meshing gears. Transmission error is a term used to describe or is defined as the differences between the theoretical and actual positions between a pinion (driving gear) and a driven gear. It has been recognized as a main source for mesh frequency excited noise and vibration. With prior knowledge of the operating conditions of the gear set it is possible to design the gears such that the vibration and noise is minimized.

Transmission error is usually due to two main factors. The first is caused by manufacturing inaccuracy and mounting errors. Gear designers often attempt to compensate for transmission error by modifying the gear teeth. The second type of error is caused by elastic deflections under load. Among the types of gearbox noise, one of the most difficult to control is gear noise generated at the tooth mesh frequency. Transmission error is considered to be one of the main contributors to noise and vibration in a gear set. This suggests that the gear noise is closely related to transmission error. If a pinion and gear have ideal involute profiles running with no loading torque they should theoretically run with zero transmission error. However, when these same gears transmit torque, the combined torsional mesh stiffness of each gear changes throughout the mesh cycle as the teeth deflect, causing variations in angular rotation of the gear body. Even though the transmission error is relatively small, these slight variations can cause noise at a frequency which matches a resonance of the shafts or the gear housing, causing the noise to be enhanced. This phenomenon has been actively studied in order to minimize the amount of transmission error in gears.

Gears analyses in the past were performed using analytical methods, which required a number of assumptions and simplifications. In general, gear analyses are multidisciplinary, including calculations related to the tooth stresses and to tribological failures such as like wear or scoring. In this thesis, static contact and bending stress analyses were performed, while trying to design spur gears to resist bending failure and pitting of the teeth, as both affect transmission error.

As computers have become more and more powerful, people have tended to use numerical approaches to develop theoretical models to predict the effect of whatever are studied. This has improved gear analyses and computer simulations. Numerical methods

can potentially provide more accurate solutions since they normally require much less restrictive assumptions. The model and the solution methods, however, must be chosen carefully to ensure that the results are accurate and that the computational time is reasonable.

The finite element method is very often used to analyze the stress state of an elastic body with complicated geometry, such as a gear. There have been numerous research studies in the area [2],[3] as described in chapter 2.

In this thesis, first, the finite element models and solution methods needed for the accurate calculation of two dimensional spur gear contact stresses and gear bending stresses were determined. Then, the contact and bending stresses calculated using ANSYS 7.1 were compared to the results obtained from existing methods. The purpose of this thesis is to develop a model to study and predict the transmission error model including the contact stresses, and the torsional mesh stiffness of gears in mesh using the ANSYS 7.1 software package based on numerical method. The aim is to reduce the amount of transmission error in the gears, and thereby reduce the amount of noise generated.

## 1.2 Objectives of the Research

In spite of the number of investigations devoted to gear research and analysis there still remains to be developed, a general numerical approach capable of predicting the effects of variations in gear geometry, contact and bending stresses, torsional mesh stiffness and transmission errors. The objectives of this thesis are to use a numerical approach to develop theoretical models of the behavior of spur gears in mesh, to help to predict the effect of gear tooth stresses and transmission error. The main focus of the current research as developed here is:

- To develop and to determine appropriate models of contact elements, to calculate contact stresses using ANSYS and compare the results with Hertzian theory.
- To generate the profile of spur gear teeth and to predict the effect of gear bending using a three dimensional model and two dimensional model and compare the results with theose of the Lewis equation.
- To determine the static transmission errors of whole gear bodies in mesh.

The objectives in the modeling of gears in the past by other researchers have varied from vibration analysis and noise control, to transmission error during the last five decades. The goals in gear modeling may be summarized as follows:

- Stress analysis such as prediction of contact stress and bending stress.
- Prediction of transmission efficiency.
- Finding the natural frequencies of the system before making the gears.
- Performing vibration analyses of gear systems.
- Evaluating condition monitoring, fault detection, diagnosis, prognosis, reliability and fatigue life.

Different analysis models will be described in chapter 2. For gears, there are many types of gear failures but they can be classified into two general groups. One is failure of the root of the teeth because the bending strength is inadequate. The other is created on the surfaces of the gears. There are two theoretical formulas, which deal with these two fatigue failure mechanisms. One is the Hertzian equation, which can be used to calculate the contact stresses. The other is the Lewis formula, which can be used to calculate the bending stresses. The surface pitting and scoring shown in Figure 1.1 [35] are the examples of failures which resulted in the fatigue failure of tooth surface. The

Hertzian equation will be used to investigate surface pitting and scoring by obtaining the magnitude of the contact stresses.

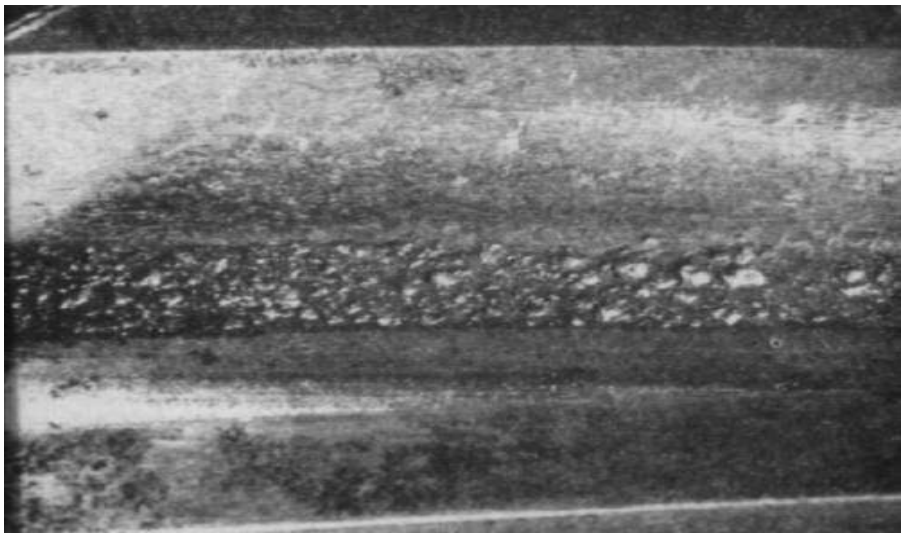

**Figure 1-1 Fatigue failure of the tooth surface**

Pitting and scoring is a phenomena in which small particles are removed from the surface of the tooth due to the high contact stresses that are present between mating teeth. Pitting is actually the fatigue failure of the tooth surface. Hardness is the primary property of the gear tooth that provides resistance to pitting. In other words, pitting is a surface fatigue failure due to many repetitions of high contact stress, which occurs on gear tooth surfaces when a pair of teeth is transmitting power.

The literature available on the contact stress problems is extensive. But that available on the gear tooth contact stress problem is small, especially for transmission error including the contact problem. Klenz [1] examined the spur gear contact and bending stresses using two dimensional FEM. Coy and Chao [9] studied the effect of the finite element grid size on Hertzian deflection in order to obtain the optimum aspect ratio at the loading point for the finite element grid. Gatcombe and Prowell [10] studied the

Hertzian contact stresses and duration of contact for a very specific case, namely a particular rocket motor gear tooth. Tsay [11] has studied the bending and contact stresses in helical gears using the finite element method with the tooth contact analysis technique. However, the details of the techniques used to evaluate the transmission error including contact stresses were not presented.

### 1.3 Layout of Thesis

This thesis is comprised of a total of six chapters. Chapter 1 presents a general introduction, and the objectives to be achieved. Finally the layout of the thesis is described. Chapter 2 is a literature review and gives background of characteristics of involute spur gears for different types of modeling. Chapter 3 describes why the contact problem is difficult. A contact problem classification was done which as well as provides a discussion of the advantages and disadvantages of contact elements. Finally a discussion on how to overcome some of the disadvantages is presented. The contact stress model between two cylinders was then developed. Many graphical results from ANSYS are shown. Chapter 4 begins with presentation of an involute gear tooth contact stress analysis model from ANSYS, and then presents the bending stresses from 3-D models and 2-D models for the different numbers of teeth. The results are compared with the results from the Lewis Formula. In Chapter 5, FEM will be used to determine the transmission error model including the contact problem for ideal involute spur gears and how to obtain the transmission error in mesh from ANSYS. Chapter 6 gives the conclusions of this thesis, and suggests future work.

# Chapter 2 Literature Review and Background

There has been a great deal of research on gear analysis, and a large body of literature on gear modeling has been published. The gear stress analysis, the transmission errors, the prediction of gear dynamic loads, gear noise, and the optimal design for gear sets are always major concerns in gear design. Errichello [12] and Ozguven and Houser[13] survey a great deal of literature on the development of a variety of simulation models for both static and dynamic analysis of different types of gears. The first study of transmission error was done by Harris [14]. He showed that the behavior of spur gears at low speeds can be summarized in a set of static transmission error curves. In later years, Mark [15] and [16] analyzed the vibratory excitation of gear systems theoretically. He derived an expression for static transmission error and used it to predict the various components of the static transmission error spectrum from a set of measurements made on a mating pair of spur gears. Kohler and Regan [17] discussed the derivation of gear transmission error from pitch error transformed to the frequency domain. Kubo et al [18] estimated the transmission error of cylindrical involute gears using a tooth contact pattern. The current literature reviews also attempt to classify gear model into groupings with particular relevance to the research. The following classification seems appropriate [64].

- Models with Tooth Compliance
- Models of Gear system Dynamics
- Models of A Whole Gearbox
- Models for Optimal Design of Gear Sets

## 2.1 Model with Tooth Compliance

These models only include the tooth deformation as the potential energy storing element in the system. There are studies of both single tooth and tooth pair models. For single tooth models, a method of stress analysis was developed. For the models with paired teeth, the contact stresses and meshing stiffness analysis usually were emphasized. The system is often modeled as a single degree of freedom spring-mass system. The basic characteristic in this group is that the only compliance considered is due to the gear tooth deflection and that all other elements have assumed to be perfectly rigid.

Harris [14] made an important contribution to this area. The importance of transmission error in gear trains was discussed and photo-elastic gear models were used in his work. Due to the loss of contact he considered manufacturing errors, variation in the tooth stiffness and non-linearity in tooth stiffness as three internal sources of vibration. Harris was the first investigator who pointed out the importance of transmission error by showing the behavior of spur gears at low speeds. His work can be summarized in a set of static transmission error curves. In 1969, Aida [67] presented other examples of studies in this area. He modeled the vibration characteristics of gears by considering tooth profile errors and pitch errors, and by including the variation of teeth mesh stiffness. In 1967, Tordion [68] first constructed a torsional multi-degree of freedom model with a gear mesh for a general rotational system. The transmission error was suggested as a new concept for determining the gear quality, rather than individual errors.

In 1981, Cornell [21] obtained a relationship between compliance and stress sensitivity of spur gear teeth. The magnitude and variation of the tooth pair compliance with load position affects the dynamics and loading significantly. The tooth root stresses

versus load varies significantly with load positions. With improved fillet/foundation compliance analysis the compliance analysis was made based on work by Weber [22] and O'Donell [23]. The stress sensitivity analysis is a modified version of the Heywood method [24]. These improved compliance and stress sensitivity analyses were presented along with their evaluation using tests, finite element analysis, and analytic transformation results, which indicated good agreement.

In 1988, Umezawa [27] developed a new method to predict the vibration of a helical gear pair. The developed simulator was created through theoretical analysis on the vibration of a narrow face width helical gear pair. The studies on a helical gear are very different from the ones on a spur gear. A simple outline of the theoretical analysis on the vibration of a helical gear is given below. The length of path of contact is on the plane of action of helical gear pairs in Figure 2.1 [27]. A pair of mated teeth starts meshing at point S on the plane of action. The meshing of the pair proceeds on the plane with the movement of the contact line. It finishes at point E, the position of the line-of-contact is represented by the coordinate Y along the line-of-action of the helical gear (hereafter simply stated as the line-of-action) which is considered to be the middle of the face width. That is, the starting point of meshing $S$ is substituted by $S^{'}$, the position of line-of-contact $CC_c$ by $C^{'}$ and the ending point $E$ by $E^{'}$ on the line-of-action. A vibration model was built [28] there. When the rotational vibration of a power-transmitting helical gear pair is considered along the line-of-action model similar to the case of a spur-gear pair, in which the tooth is replaced by a spring and the gear blank is replaced by a mass.

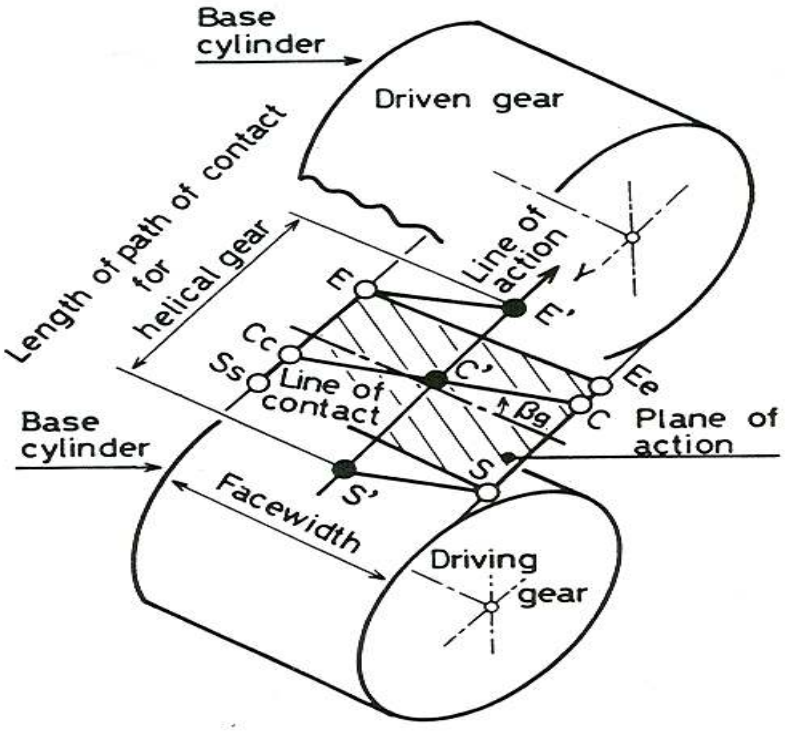


**Figure 2-1 Meshing of a helical pair**

In 1992, Vijayarangan and Ganesan [58] studied static contact stresses including the effect of friction between the mating gear teeth. Using the conventional finite element method the element stiffness matrices and the global stiffness matrix $[K]$ of the two gears in mesh were obtained. If the external forces at the various nodes are known, then the system of equations is written as:

$$[K]\{U\} = \{F\} \tag{2.1}$$

where $\{U\}$ is the nodal displacement vector and $\{F\}$ is the nodal force vector. The system of equations is solved and $\{U\}$ is obtained. Then the stress can be calculated. Each gear is divided into a number of elements such that in the assumed region of contact there is equal number of nodes on each gear. These contact nodes are all grouped together.

In 2001, David and Handschuh [20] investigated the effect of this moving load on crack trajectories. The objective of this work was to study the effect of the moving gear tooth load on crack propagation predictions. A finite element model of a single tooth was used to analyze the stress, deformation and fracture in gear teeth when subjected to dynamic loading. At different points on the tooth surface impulsive loads were applied. Moving loads normal to the tooth profile were studied. Even effective designs have the possibility of gear cracks due to fatigue. In addition, truly robust designs consider not only crack initiation, but crack propagation trajectories. As an example, crack trajectories that propagate through the gear tooth are the preferred mode of failure compared to propagation through the gear rim. Rim failures would lead to catastrophic events and should be avoided. Analysis tools that predict crack propagation paths can be a valuable aid to the designer to prevent such catastrophic failures. Using weighting function techniques to estimate gear tooth stress intensity factors, analytical methods have been developed [53]. Numerical techniques such as the boundary element method and the finite element method have also been studied [54]. Based on stress intensity factors, and fatigue crack growth, gear life predictions have been investigated [55]. The gear crack trajectory predictions have been addressed in a few studies [56]. From publications on gear crack trajectory predictions, the analytical methods have been used in numerical form (finite or boundary element methods) while solving a static stress problem.

## 2.2 Models of Gear System Dynamics

The current models can predict shaft torsional vibration, shaft bending stiffness, gear tooth bending stiffness, bearings stiffness, etc. The models of gear system dynamics include the flexibility of the other parts as well as the tooth compliance. The flexibility of

shafts and the bearings along the line of action are discussed. In these models, the torsional vibration of the system is usually considered.

In 1971, Kasuba [66] determined dynamic load factors for gears that were heavily loaded based on one and two degree of freedom models. Using a torsional vibratory model, he considered the torsional stiffness of the shaft. In 1981, he published another paper [48]. An interactive method was developed to calculate directly a variable gear mesh stiffness as a function of transmitted load, gear profile errors, gear tooth deflections and gear hub torsional deformation, and position of contacting profile points. These methods are applicable to both normal and high contact ratio gearing. Certain types of simulated sinusoidal profile errors and pitting can cause interruptions of the normal gear mesh stiffness function, and thus, increase the dynamic loads. In his research, the gear mesh stiffness is the key element in the analysis of gear train dynamics. The gear mesh stiffness and the contact ratio are affected by many factors such as the transmitted loads, load sharing, gear tooth errors, profile modifications, gear tooth deflections, and the position of contacting points.

In 1979 Mark [15] [16] analyzed the vibration excitation of gear systems. In his papers, formulation of the equations of motion of a generic gear system in the frequency domain is shown to require the Fourier-series coefficients of the components of vibration excitation. These components are the static transmission errors of the individual pairs in the system. A general expression for the static transmission error is derived and decomposed into components attributable to elastic tooth deformations and to deviations of tooth faces from perfect involute surfaces with uniform lead and spacing.

In the 1980s although more and more advanced models were developed in order to obtain more accurate predictions, some simple models were developed for the purpose

of simplifying dynamic load prediction for standard gears. In 1980, the coupled torsional-flexural vibration of a shaft in a spur geared system was investigated by some researchers. That the output shaft was flexible in bearing and the input shaft was rigid in bearing was assumed. Researchers derived equations of motion for a 6-degree-of-freedom (DOF) system. The tooth contact was maintained during the rotation and the mesh was rigid in those models. Four years later, other researchers presented another model that consists of three shafts, rather than two shafts, one of them being a counter shaft.

In 1992, Kahraman [41] developed a finite element model of a geared rotor system on flexible bearings. The gear mesh was modeled by a pair of rigid disks connected by a spring and a damper with a constant value which represented the average mesh value. Coupling between the torsional and transverse vibrations of the gear was considered in the model, and applied the transmission error as the excitation at the mesh point to simulate the variable mesh stiffness.

In 1996, Sweeney [25] developed a systematic method of calculating the static transmission error of a gear set, based on the effects of geometric parameter variation on the transmission error. He assumed that the tooth (pair) stiffness is constant along the line of action (thin-slice model) and that the contact radius for calculation of Hertzian deformation is the average radius of the two profiles in contact. Sweeney's model is applicable to cases where the dominant source of transmission error is geometric imperfections, and is particularly suited to automotive quality gear analysis. The results of his model gave very good agreement with measurements on automotive quality gears.

Randall and Kelley [26] modifications have been made to Sweeney's basic model to extend it to higher quality gears where the tooth deflection component is more

important. The tooth deflection compliance matrix and the contact compliance vector have been derived using finite element models. The effects on the transmission error of the variation of the tooth body stiffness with the load application point have been investigated, and a simulation program for transmission error (TE) computation with varying stiffness has been developed. In order to study the case where the tooth deflection component is the dominant source of the transmission error nylon gears were used. All the simulation results have been compared with the measured transmission errors from a single-stage gearbox.

In 1999, Kelenz [1] investigated a spur gear set using FEM. The contact stresses were examined using a two dimensional FEM model. The bending stress analysis was performed on different thin rimmed gears. The contact stress and bending stress comparisons were given in his studies.

In 2001, Howard [34] simplified the dynamic gear model to explore the effect of friction on the resultant gear case vibration. The model which incorporates the effect of variation in gear tooth torsional mesh stiffness, was developed using finite element analysis, as the gears mesh together. The method of introducing the frictional force between teeth into the dynamic equations is given in his paper. The comparison between the results with friction and without friction was investigated using Matlab and Simulink models developed from the differential equations.

In 2003, Wang [7] surveyed the nonlinear vibration of gear transmission systems. The progress in nonlinear dynamics of gear driven system is reviewed, especially the gear dynamic behavior by considering the backlash and time-varying mesh stiffness of teeth. The basic concepts, the mathematical models and the solution methods for non-linear dynamics of geared systems were all reviewed in his paper.

## 2.3 Models of a Whole Gearbox

The studies in this group may be thought of as advanced studies. Traditional analysis approaches mentioned previously in the gear dynamic area have concentrated on the internal rotating system and have excluded dynamic effects of the casing and flexible mounts. All elements in the system including the gear casing are considered in the recent models. The studies of this group is to focus on the dynamic analysis including the gear pair, shafts, rolling element bearings, a motor, a load, a casing and a flexible or rigid mount. The gearbox may be single stage or multi-stage.

In 1991, Lim and Singh [38] presented study of the vibration analysis for complete gearboxes. Three example cases were given there: a single-stage rotor system with a rigid casing and flexible mounts, a spur gear drive system with a rigid casing and flexible mounts, and a high-precision spur gear drive system with a flexible casing and rigid mounts. In 1994, Sabot and Perret-Liaudet [57] presented another study for noise analysis of gearboxes. A troublesome part of the noise within the car or truck cab could be attributed by the transmission error which gives rise to dynamic loads on teeth, shafts, bearings and the casing. During the same year, a simulation method by integrating finite element vibration analysis was developed by others. Each shaft was modeled as a lumped mass and added to the shaft in their model. Each of the rolling element bearings was represented as a spring and damper. The casing of the gearbox was modeled by a thin shell element in the finite element package program.

## 2.4 Models for Optimal Design of Gear Sets

Several approaches to the models for optimum design of gears have been presented in the recent literature. Cockerham [29] presents a computer design program for 20-degree pressure angle gearing, which ignores gear-tooth-tip scoring. This program

varies the diametral pitch, face width, and gear ratio to obtain an acceptable design. Tucker [30] and Estrin [31] look at the gear mesh parameters, such as addendum ratios and pressure angles and outline the procedures for varying a standard gear mesh to obtain a more favorable gear set. Gay [32] considers gear tip scoring and shows how to modify a standard gear set to bring this mode of failure into balance with the pitting fatigue mode. In order to obtain an optimal design he adjusts the addendum ratios of the gear and pinion. The basic approach available is to check a given design to verify its acceptability [33], [36] to determine the optimal size of a standard gear mesh. With the object of minimizing size and weight, optimization methods are presented for the gearbox design [37], [39]. The gear strengths must be considered including fatigue as treated by the AGMA (American Gear Manufacturing Association) [40]. Surface pitting of the gear teeth in the full load region must also be handled with [43]-[45] as scoring at the tip of the gear tooth [46], [47].

In 1980, Savage and Coy [19] optimized tooth numbers for compact standard spur gear sets. The design of a standard gear mesh was treated with the objective of minimizing the gear size for a given gear ratio, pinion torque, and the allowable tooth strength. Scoring, pitting fatigue, bending fatigue, and interference are considered. A design space is defined in terms of the number of teeth on the pinion and the diametric pitch. This space is then combined with the objective function of minimum center distance to obtain an optimal design region. This region defines the number of pinion teeth for the most compact design.

Many engineering design problems are multiobjective as they often involve more than one design goal to be optimized. These design goals impose potentially conflicting requirements on the technical and cost reduction performances of system design. To

study the trade-offs that exist between these conflicting design goals and to explore design options, one needs to formulate the optimization problem with multiple objectives. The optimization algorithms seek an optimum design, which attains the multiple objectives as closely as possible while strictly satisfying constraints. To help the exploration of different multiobjective formulations Stadler and Dauer [49] incorporated Pareto optimality concepts into the optimization algorithms, which require the designer's involvement as a decision maker. A variety of techniques and many applications of multiobjective optimization have been developed over the past few years. Tappeta [51] and Hwang and Masud [50] summarized the progress in the field of multi-criteria optimization. A comprehensive survey of multiobjective optimization methods is also given. The most traditional methods involve converting a multiobjective problem into a single objective problem for a compromise solution are also presented. This scalarization was usually achieved using either weights or targets that the designers have to specify for each objective a priori. Some of the disadvantages of traditional methods are listed there [52].

In 2001, Chong and Bar [8] demonstrated a multiobjective optimal design of cylindrical gear pairs for the reduction of gear size and meshing vibration. The results of the relation between the geometrical volume and the vibration of a gear pair were analyzed, in addition a design method for cylindrical gear pairs to balance the conflicting objectives by using a goal programming formulation was proposed. The design method reduces both the geometrical volume and the meshing vibration of cylindrical gear pairs while satisfying strength and geometric constraints.

# Chapter 3 Contact Stress Simulation of Two Cylinders

## 3.1 Why is the Contact Problem Significantly Difficult

Despite the importance of contact in the mechanics of solids and its engineering applications, contact effects are rarely seriously taken into account in conventional engineering analysis, because of the extreme complexity involved. Mechanical problems involving contacts are inherently nonlinear. Why is it "nonlinear" behavior? Usually the loading causes significant changes in stiffness, which results in a structure that is nonlinear. Nonlinear structural behavior arises for a number of reasons, which can be reduced to three main categories: (1) Geometric Nonlinearities (Large Strains, Large Deflections) (2) Material Nonlinearities (Plasticity) (3) Change in Status Nonlinearities (Contact). So the contact between two bodies belongs to the case (3).

Why is the contact problem significantly difficult? Contact problems present many difficulties. First, the actual region of contact between deformable bodies in contact is not known until the solution has been obtained. Depending on the loads, materials, and boundary conditions, along with other factors, surfaces can come into and go out of contact with each other in a largely unpredictable manner. Secondly, most contact problems need to account for friction. The modeling of friction is very difficult as the friction depends on the surface smoothness, the physical and chemical properties of the material, the properties of any lubricant that might be present in the motion, and the temperature of the contacting surfaces. There are several friction laws and models to choose from, and all are nonlinear. Frictional response can be chaotic, making solution convergence difficult (ANSYS). In addition to those difficulties, many contact problems must also address multi-field effects, such as the conductance of heat and electrical

currents in the areas of contact. Bodies in contact may have complicated geometries and material properties and may deform in a seemingly arbitrary way.

With the rapid development of computational mechanics, however, great progress has been made in numerical analysis of the problem. Using the finite element method, many contact problems, ranging from relatively simple ones to quite complicated ones, can be solved with high accuracy. The Finite Element Method can be considered the favorite method to treat contact problems, because of its proven success in treating a wide range of engineering problem in areas of solid mechanics, fluid flow, heat transfer, and for electromagnetic field and coupled field problems.

## 3.2 How to Solve the Contact Problem

### 3.2.1 Contact Problem Classification

There are many types of contact problems that may be encountered, including contact stress, dynamic impacts, metal forming, bolted joints, crash dynamics, assemblies of components with interference fits, etc. All of these contact problems, as well as other types of contact analysis, can be split into two general classes (ANSYS),

Rigid - to - flexible bodies in contact,

Flexible - to - flexible bodies in contact.

In rigid - to - flexible contact problems, one or more of the contacting surfaces are treated as being rigid material, which has a much higher stiffness relative to the deformable body it contacts. Many metal forming problems fall into this category. Flexible-to-flexible is where both contacting bodies are deformable. Examples of a flexible-to-flexible analysis include gears in mesh, bolted joints, and interference fits.

### 3.2.2 Types of Contact Models

In general, there are three basic types of contact modeling application as far as ANSYS use is concerned.

Point-to-point contact: the exact location of contact should be known beforehand. These types of contact problems usually only allow small amounts of relative sliding deformation between contact surfaces.

Point-to-surface contact: the exact location of the contacting area may not be known beforehand. These types of contact problems allow large amounts of deformation and relative sliding. Also, opposing meshes do not have to have the same discretisation or a compatible mesh. Point to surface contact was used in this chapter.

Surface-to-surface contact is typically used to model surface-to-surface contact applications of the rigid-to-flexible classification. It will use in chapter 5.

### 3.2.3 How to Solve the Contact Problem

In order to handle contact problems in meshing gears with the finite element method, the stiffness relationship between the two contact areas is usually established through a spring that is placed between the two contacting areas. This can be achieved by inserting a contact element placed in between the two areas where contact occurs.

There are two methods of satisfying contact compatibility: (i) a penalty method, and (ii) a combined penalty plus a Lagrange multiplier method. The penalty method enforces approximate compatibility by means of contact stiffness. The combined penalty plus Lagrange multiplier approach satisfies compatibility to a user-defined precision by the generation of additional contact forces that are referred to as Lagrange forces.

It is essential to prevent the two areas from passing through each other. This method of enforcing contact compatibility is called the penalty method. The penalty allows surface penetrations, which can be controlled by changing the penalty parameter of the combined normal contact stiffness. If the combined normal contact stiffness is too small, the surface penetration may be too large, which may cause unacceptable errors. Thus the stiffness must be big enough to keep the surface penetrations below a certain level. On the other hand, if the penalty parameter is too large, then the combined normal contact stiffness may produce severe numerical problems in the solution process or simply make a solution impossible to achieve. For most contact analyses of huge solid models, the value of the combined normal contact stiffness may be estimated [ANSYS] as,

$$k_n \approx fEh \tag{3.1}$$

where $f$ is a factor that controls contact compatibility. This factor is usually be between 0.01 and 100,

$E =$ smallest value of Young's Modulus of the contacting materials

$h =$ the contact length

The contact stiffness is the penalty parameter, which is a real constant of the contact element. There are two kinds of contact stiffness, the combined normal contact stiffness and the combined tangential or sticking contact stiffness. The element is based on two stiffness values. They are the combined normal contact stiffness $k_n$ and the combined tangential contact stiffness $k_t$. The combined normal contact stiffness $k_n$ is used to penalize interpenetration between the two bodies, while the combined tangential contact stiffness $k_t$ is used to approximate the sudden jump in the tangential force, as

represented by the Coulomb friction when sliding is detected between two contacting nodes. However, serious convergence difficulties may exist during the vertical loading process and application of the tangential load often results in divergence. A detailed examination of the model's nodal force during the vertical loading may indicate the problem. Not only are friction forces developing but they develop in random directions. This is due to Poission's effect causing small transverse deflections of the nodes in the contact zone. These deflections are enough to activate the friction forces of the contact elements [1]. The friction forces are developing in various directions because the generation of a tangential friction force facing right on one node would tend to pull the node on its left to the right. This would generate a friction force facing left on this node, pulling back on the other node. This continual tug-of-war causes the poor convergence. This problem was eliminated by applying a small rotation to the above cylinder model forces as it was displaced and loaded vertically. This rotation ensured that the friction forces would develop in the proper direction.

The contact problem is addressed using a special contact element. A number of contact elements were available (two and three dimensional, spring and damper combinations). For the problem in hand, the element to be used is a two-dimensional, the three nodes, and point-to-surface contact element. In the input file, the CONTAC48 element from the ANSYS element library as the contact elements between the two contact bodies shown as Figure 3.1 was chosen. It is applicable to 2-D geometry, plane strain, plane stress, or axisymmetry situations. The area of contact between two or more bodies is generally not known in advance. It may be applied to the contact of solid bodies for static or dynamic analyses, to problems with or without friction, and to flexible-to-flexible or rigid-to-flexible body contact.

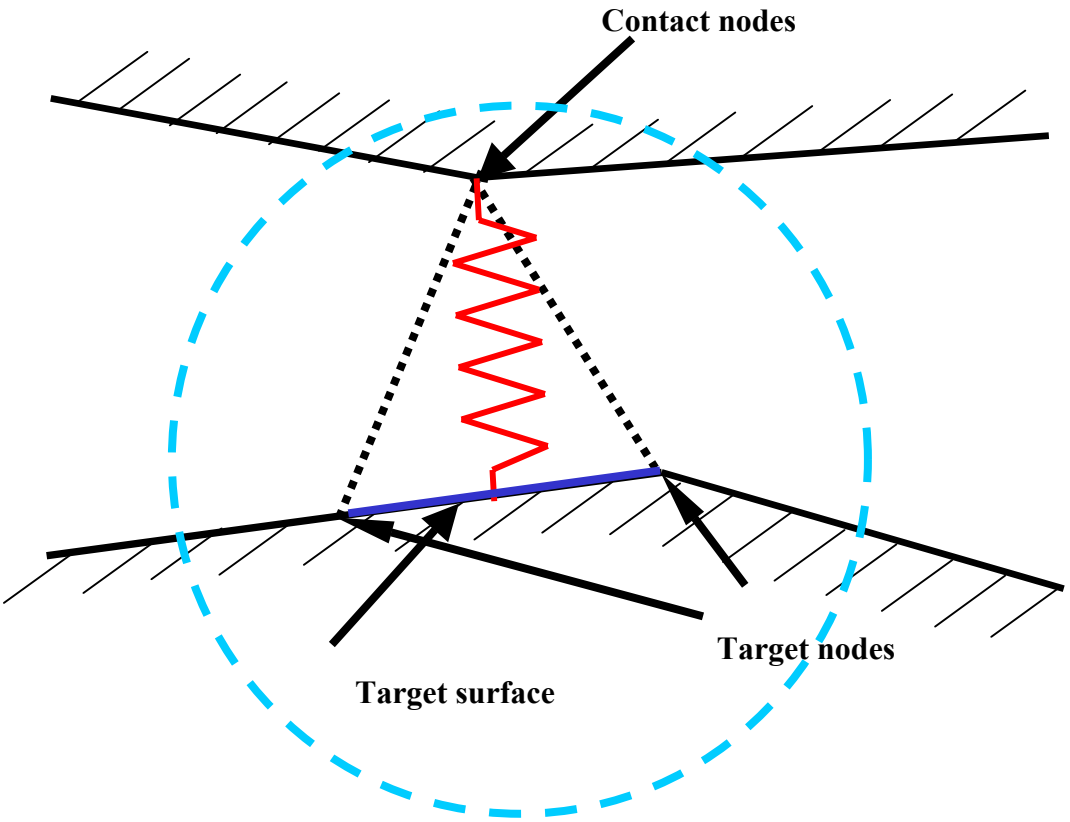


**Figure 3-1 Point-to-surface contact element**

### 3.2.4 Contact Element Advantages, Disadvantages and their Convergence

Because of the simplicity of their formulation, the advantages of using contact elements are:

- They are easy to use
- They are simple to formulate, and
- They are easily accommodated into existing FE code.

However, using contact elements poses some difficulties such as the fact that their performance, in term of convergence and accuracy, depends on user defined parameters.

In overcoming convergence difficulties, usually the biggest challenge is that the solution must start within the radius of convergence. However, there is no simple way to determine the radius of convergence. If the solution converges, the start was within the radius. If solution fails to converge, the start was outside the radius. Trial-and-error must be used to obtain convergence. In order to get convergence in ANSYS, difficult problems might require many load increments, and if many iterations are required, the overall solution time increases. Balancing expense versus accuracy: All FEA involves a trade-off between expense and accuracy. More detail and a finer mesh generally leads to a more accurate solution, but requires more time and system resources. Nonlinear analyses add an extra factor, the number of load increments, which affect both accuracy and expense. Other nonlinear parameters, such as contact stiffness, can also affect both accuracy and expense. One must use their own engineering judgment to determine how much accuracy is needed versus how much expense can be afforded.

### 3.2.5 Numerical Example ---- Contact Problem of Two Circular Discs

First, to investigate the accuracy of the present method, two circular elastic discs under two-dimensional contact are analysed, and the numerical solutions are compared with that of the Hertz theory. The calculation is carried out under a plane strain condition with a Poisson's ratio of 0.3 using eight-node isoparametric elements.

Consider two circular discs, A and B, with a radius of R1= 3 in. and R2= 3 in. as shown in Figure 3.2. To reduce the number of nodes and elements and to save more computer memory space, half of the discs are partitioned to the finite element mesh, the number of elements and nodes for each disc is 1766 and 1281, respectively.

In this problem, two steel cylinders are pressed against each other. This model was built based on the Hertz contact stress theoretical problem. The radii were calculated from the pitch diameters of the pinion and gear and other parameters shown in Table 3.1 and Figure 3.2. The contact stress of this model should represent the contact stress between two gears. In the input file, first, the geometry of two half cylinders, must be described. Then the geometry areas were meshed. In contact areas a fine mesh was built. The boundary conditions were applied in this model. The loads also were applied four times as four steps. In each step there are a lot of sub-steps. In each sub-step the number of equilibrium iterations was set. The steel material properties have an elastic Young's modulus of 30,000,000 psi and the Poisson's ratio was 0.30.

**Table 3.1 Specifications of spur gears used**

| | |
|---|---|
| Number of teeth | 25 |
| Normal Module (M) | 6 mm |
| Addendum Modification coefficient | 0 |
| Normal Pressure Angle | 20 degrees |
| Face Width (mm) | 0.015 M |
| Addendum (mm) | 1.00 M |
| Dedendum (mm) | 1.25 M |

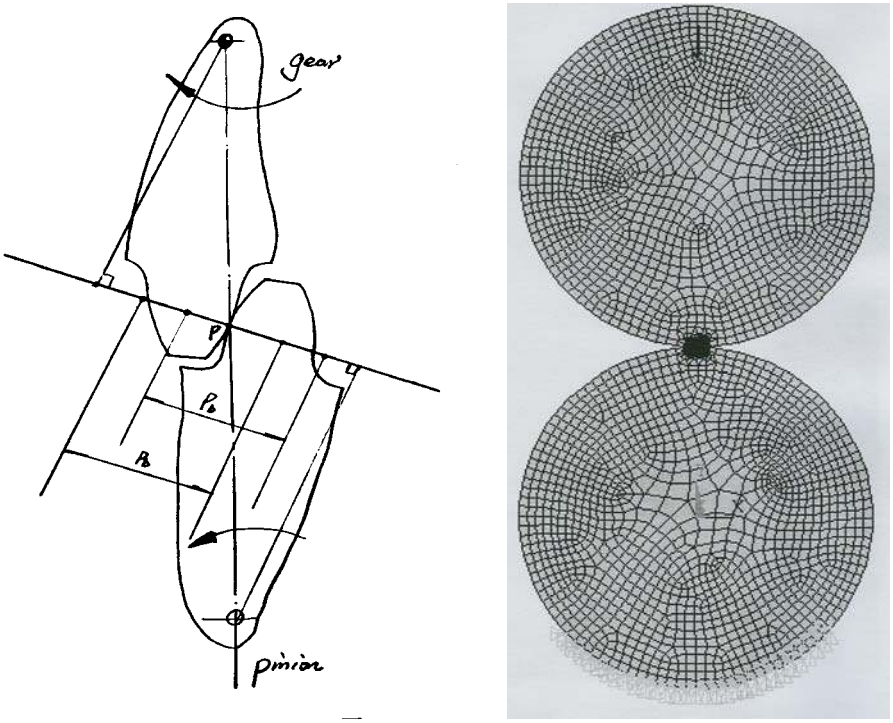


**Figure 3-2 Two steel cylinders are pressed against each other**

### 3.2.6 The FEM Numerical Procedure

The resulting contact problem is highly nonlinear and usually requires significant computer resources to solve. Contact nonlinearities occur when two components come into or out of contact with each other or when two components slide relative to each other. This nonlinear contact problem can be simulated using the FEA method. It can use the linear problem iterated many times instead of solving the nonlinear problem. That means that the nonlinear problem is usually solved based on the linear problem. For a linear elastic problem, in the 1600s, Robert Hooke discovered a simple linear relationship between force $\{F\}$ and displacement {u}:

$$\{K\}\{u\} = \{F\} \tag{3.2}$$

where $\{K\}$ is the stiffness matrix, and represents structural stiffness,

$\{u\}$ is the displacement vector, and

$\{F\}$ is the applied load vector.

A linear structure obeys this linear relationship. A common example is a simple spring. Linear structures are well suited to finite-element analysis, which is based on linear matrix algebra. If $\{K\}$ is constant and known, the problem can be solved for $\{u\}$ using a linear equation solver. However, significant classes of structures do not have a linear relationship between force and displacement. Because a plot of $F$ versus $u$ for such structures is not a straight line, such structures are said to be nonlinear. The stiffness is no longer a constant $K$. It becomes a function of applied load. In a nonlinear analysis, the response cannot be predicted directly with a set of linear equations. However, a nonlinear structure can be analyzed using an iterative series of linear approximations, with corrections. For example in modeling most contact problems, the contact area is not known in advance, $\{K\}$ is a function of $\{u\}$ and an iterative procedure is needed. ANSYS uses an iterative process called the Newton-Raphson method which functions as follows:

$$\{K(u_{i-1})\}\{u_i\} = \{F\} \tag{3.3}$$

Where $\{u_{i-1}\}$ is known, the deflection $\{u_i\}$ is calculated by Gaussian elimination. For example, using the stiffness of the undeflected shape, the deflections $\{u_1\}$ are calculated. Each iteration is known as an equilibrium iteration. Since the stiffness of the structure in the displaced configuration is different than in the previous configuration[1], the applied load and structure's reaction force are not in equilibrium. The Newton Raphson method uses this force imbalance to drive the structure to equilibrium. A full Newton-Raphson iterative analysis for one increment of load and four iterations is shown as Figure 3.3. In Figure 3.3 the relationship is shown between the loads and the displacement when the linear problem is used instead of the nonlinear problem.

In other words, the Finite Element Method treats contact problems by extending the variational formulation upon which the Finite Element Method is based. The stiffness matrix associated with contact elements and other element stiffness matrices of the body are formulated and assembled into the original finite element model. The solution is then obtained by solving the resulting set of nonlinear equations.

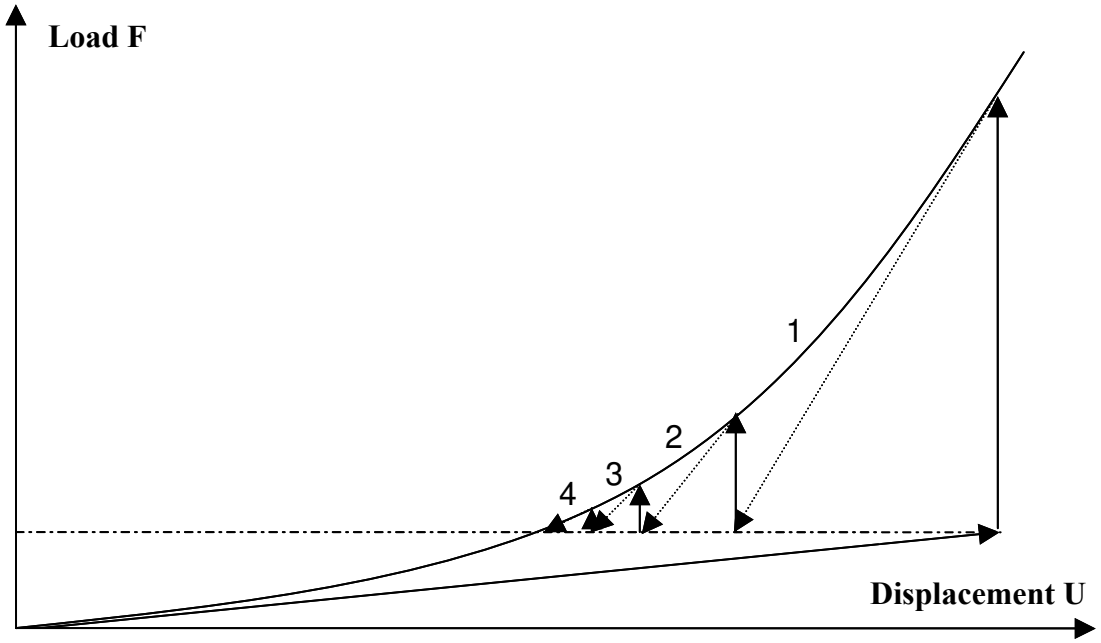


Figure 3-3 Equilibrium iteration

### 3.3 Hertz Contact Stress Equations

Usually, the current methods of calculating gear contact stresses use Hertz's equations, which were originally derived for contact between two cylinders. Contact stresses between two cylinders were shown in Figure 3.4. An ellipsoidal-prism pressure distribution is generated between the two contact areas.

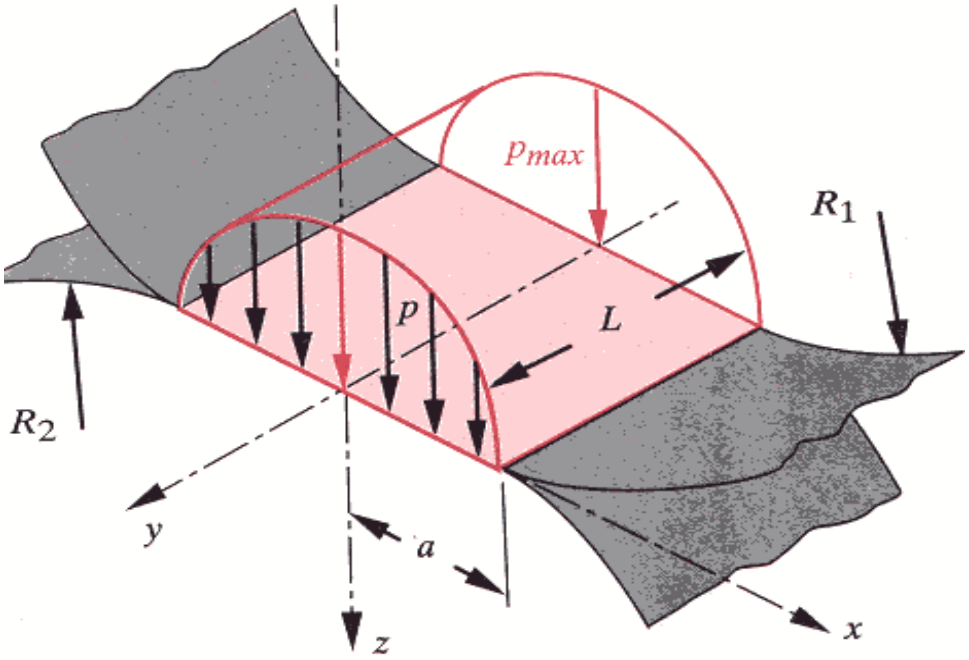


**Figure 3-4 Ellipsoidal-prism pressure distribution**

From Figure 3.4 the width of the contact zone is 2a. If total contact force is F and contact pressure is p(x), there is a formula [5], which shows the relationship between the force F and the pressure p(x):

$$F = 2L\int_0^a p(x)\,dx \quad , \tag{3.4}$$

$$\text{Contact width } a = \sqrt{\frac{2F}{\pi L}\frac{(1-\upsilon_1^{\,2})/E_1 + (1-\upsilon_2^{\,2})/E_2}{1/d_1 + 1/d_2}} \quad , \tag{3.5}$$

$$\text{The maximum contact stress } P_{\max} = \frac{2F}{\pi a L} \, , \tag{3.6}$$

$d_1$ and $d_2$ represent the pinion and gear pitch diameters.

The maximum surface (Hertz) stress:

$$P_{\max} = \sigma_H = 0.564 \sqrt{\frac{F\left(\frac{1}{R_1} + \frac{1}{R_2}\right)}{\frac{1-\upsilon_1^2}{E_1} + \frac{1-\upsilon_2^2}{E_2}}} \tag{3.7}$$

$F$ is the load per unit width,

$R_i$ is the radius of cylinder $i$, $R_i = d_i \sin\varphi/2$ for the gear teeth,

$\varphi$ is pressure angle, $\upsilon_i$ is Poisson's ratio for cylinder $i$,

$E_i$ is Young's modulus for cylinder $i$.

### 3.4 The Result of the Contact Stress Analysis

The objective of the contact stress analyses was to gain an understanding of the modeling and solution difficulties in contact problems and examine the contact stresses in the gears. In order to verify the FEM contact model procedure, contact between two cylinders was modeled. To reduce computer time, only half cylinders were meshed in the model as shown in Figure 3.5(a). The fine meshed rectangular shaped elements were generated near contact areas shown as 3.5 (b). The dimensions of the elements are based on the half width of the contact area. The contact conditions are sensitive to the geometry of the contacting surfaces, which means that the finite element mesh near the contact zone needs to be highly refined. Finer meshing generally leads to a more accurate solution, but requires more time and system resources. It is recommended not to have a fine mesh everywhere in the model to reduce the computational requirements. The edge length $dx$ of the rectangular shaped fine mesh elements: $dx = 2 * a / Num.$ $Num$ is the number of elements in the contact zone as specified in the input file. It was hoped that the

number of elements in the Hertz contact zone could be related to the solution accuracy, independent of the specific force or cylinder sizes considered. *Num* is equal to 10 here.

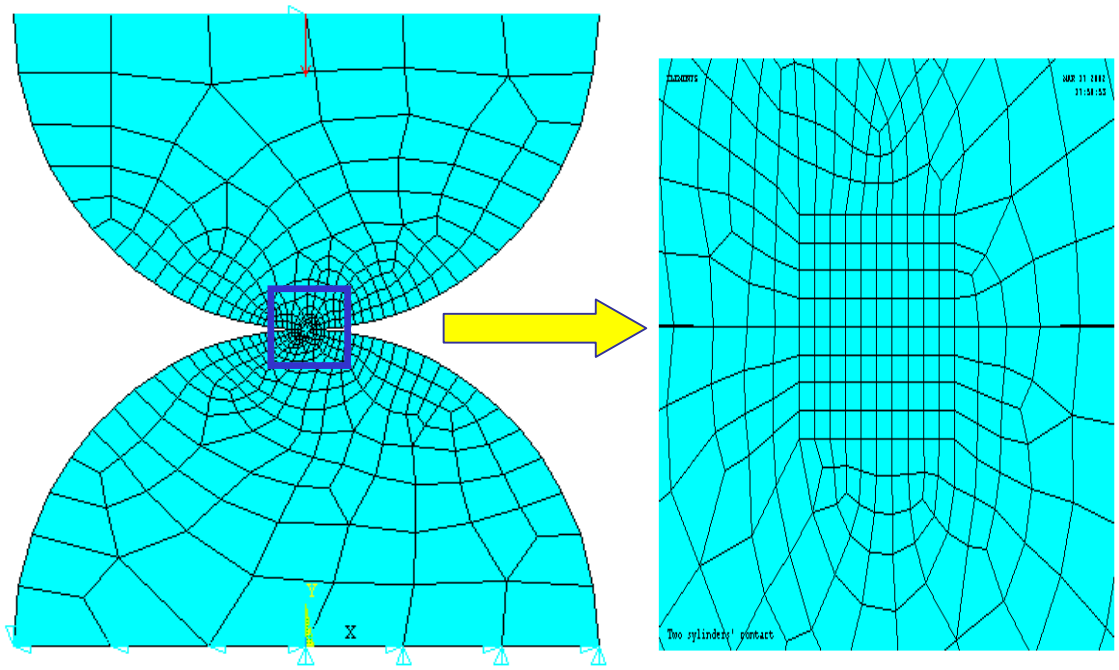


(*a*) (*b*)

**Figure 3-5 Rectangular shaped elements were generated near contact areas**

The normal contact stress along the contact surface from the ANSYS solution is shown in Figure 3.6. Figure 3.6 (a) and (b) show the distributions of the contact stress along the contact area, and Figure 3.6 (c) shows the magnitude directly from ANSYS.

The comparison of results from FEM and the Hertzian theoretical formula are shown in Figure 3.7 in which the two distributions lie very close. The red color line represents the value from the theoretical Hertz equation and the blue color points represent the results from ANSYS. They match very well. It is easy to see the blue color points are on the red curve.

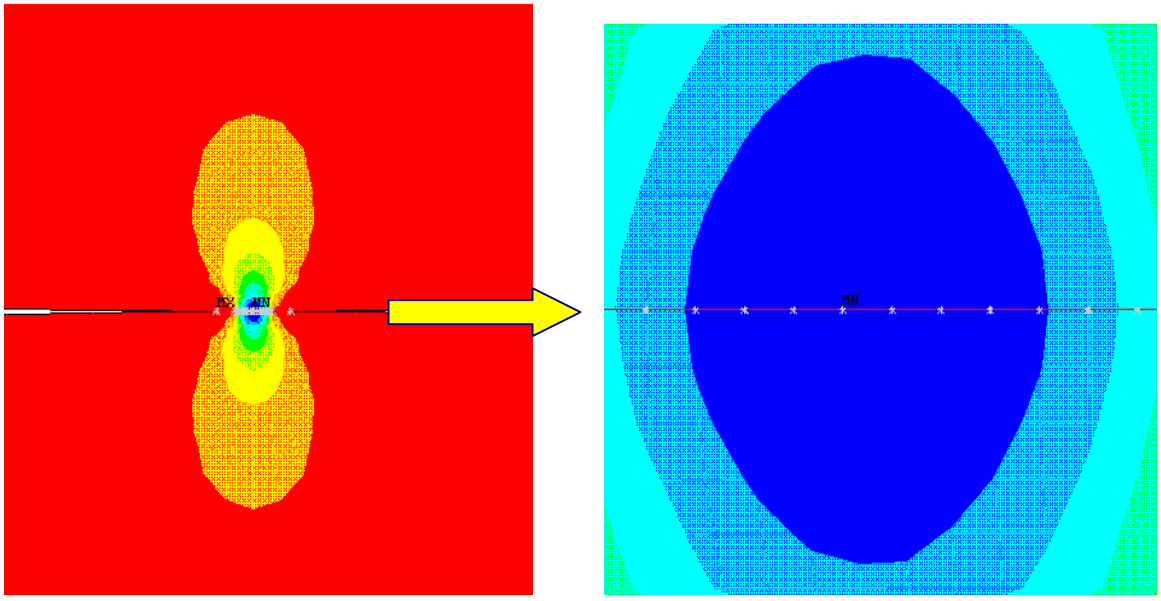

**(a)** **(b)**

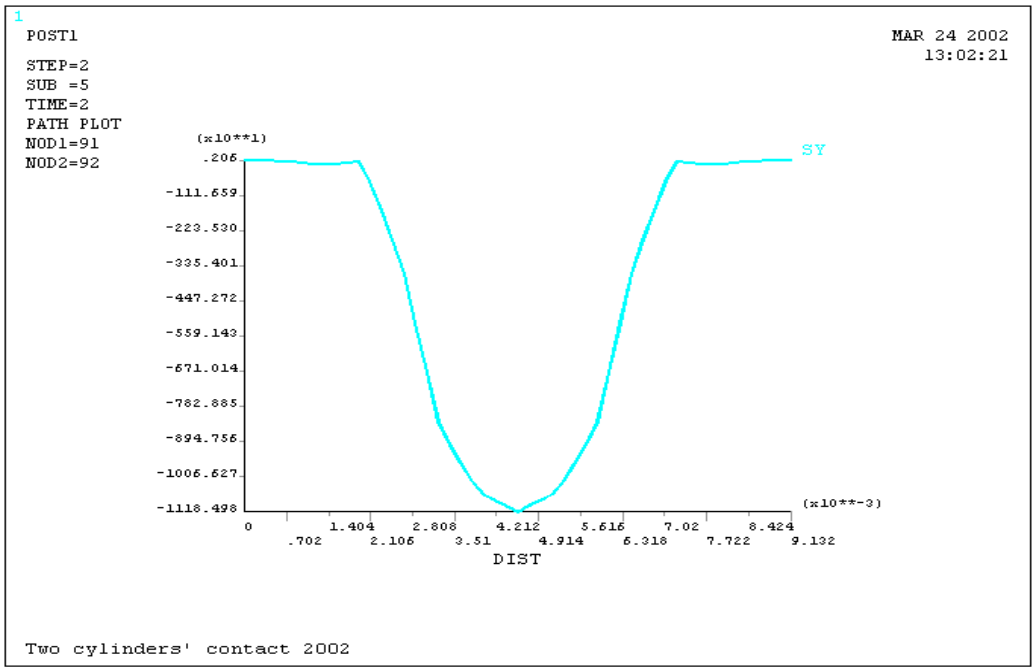


**(c)**

**Figure 3-6 Normal contact stress along the contact surface**

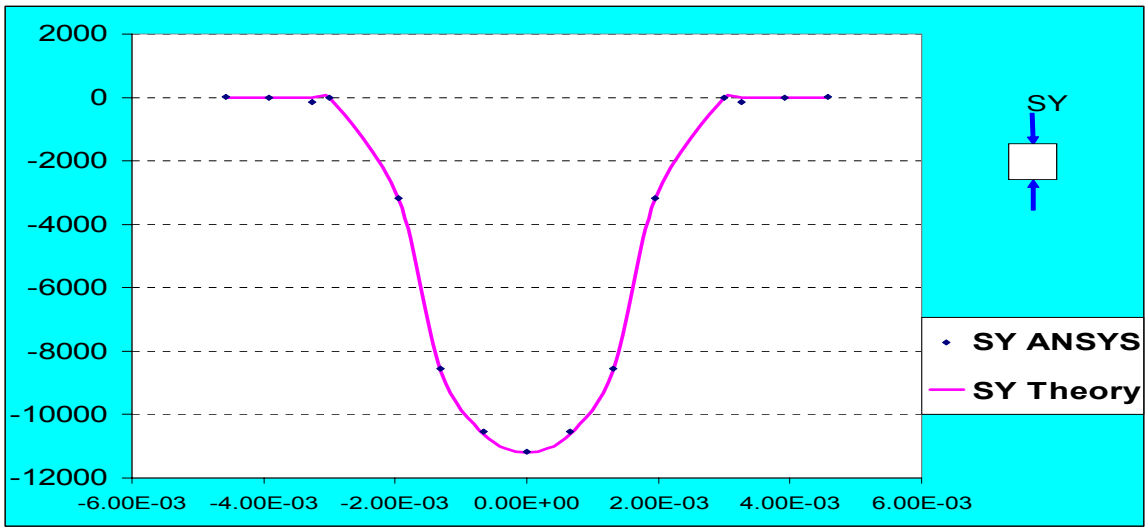


**Figure 3-7 Contact stress from ANSYS agrees with the Hertz stress**

Figure 3.8 shows the stresses $\sigma_x, \sigma_y$ as a function of depth y along a radius of the cylinder. The depth is normalized to the half-width $a$ of the contact patch. This plot provides a dimensionless picture of the stress distribution on the centerline under an ellipsoidal contact. Note all the stresses have diminished to <10% of $P_{\max}$ within $y = 5a$.

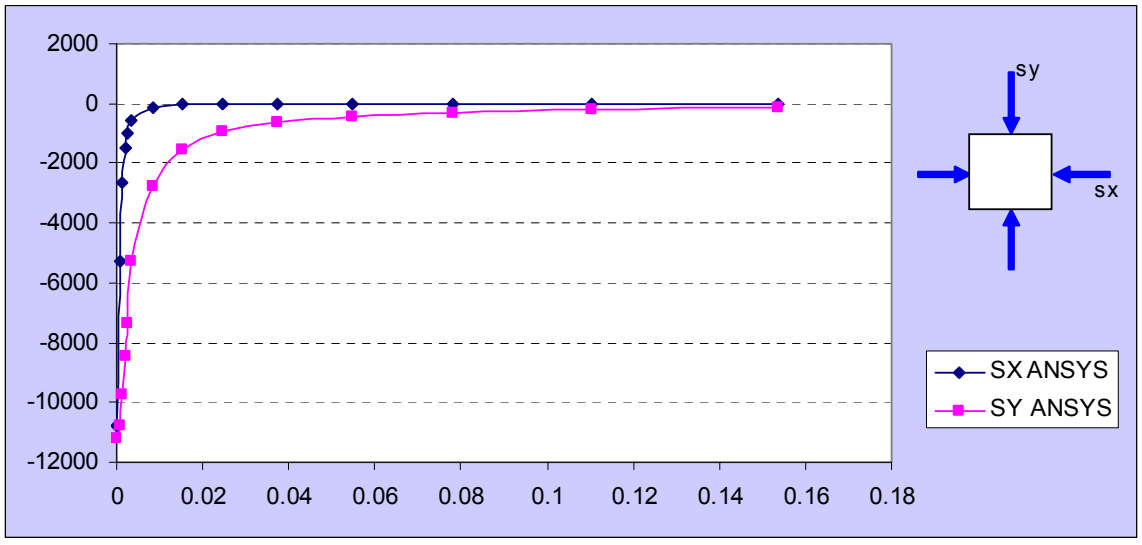


**Figure 3-8 Stress along depth distance below the contact surface from ANSYS**

The blue colour curve represents stress in the x direction, and the red color curve represents the stress in the y direction. Both of these stresses distributions are along the depth distance, which is perpendicular to contact surface. The next step is to compare results from ANSYS with the results from the theoretical equations. The stresses due to the normal loading $F_{\max}$ are [1]

$$\sigma_x = -\frac{y}{\pi}\left[\frac{a^2 + 2x^2 + 2y^2}{a}\beta - \frac{2\pi}{a} - 3x\alpha\right]F_{\max} \tag{3.8}$$

$$\sigma_y = -\frac{y}{\pi}[a\beta - x\alpha]F_{\max} \tag{3.9}$$

$$\tau_{xy} = -\frac{1}{\pi}y^2\alpha F_{\max} \tag{3.10}$$

where the factors $\alpha$ and $\beta$ are given by

$$\alpha = \frac{\pi}{k_1}\frac{1 - \sqrt{\frac{k_2}{k_1}}}{\sqrt{\frac{k_2}{k_1}}\sqrt{2\sqrt{\frac{k_2}{k_1}} + \left(\frac{k_1 + k_2 - 4a^2}{k_1}\right)}} \tag{3.11}$$

$$\beta = \frac{\pi}{k_1}\frac{1 + \sqrt{\frac{k_2}{k_1}}}{\sqrt{\frac{k_2}{k_1}}\sqrt{2\sqrt{\frac{k_2}{k_1}} + \left(\frac{k_1 + k_2 - 4a^2}{k_1}\right)}} \tag{3.12}$$

$$\begin{aligned} k_1 &= (a + x)^2 + y^2 \\ k_2 &= (a - x)^2 + y^2 \end{aligned} \tag{3.13}$$

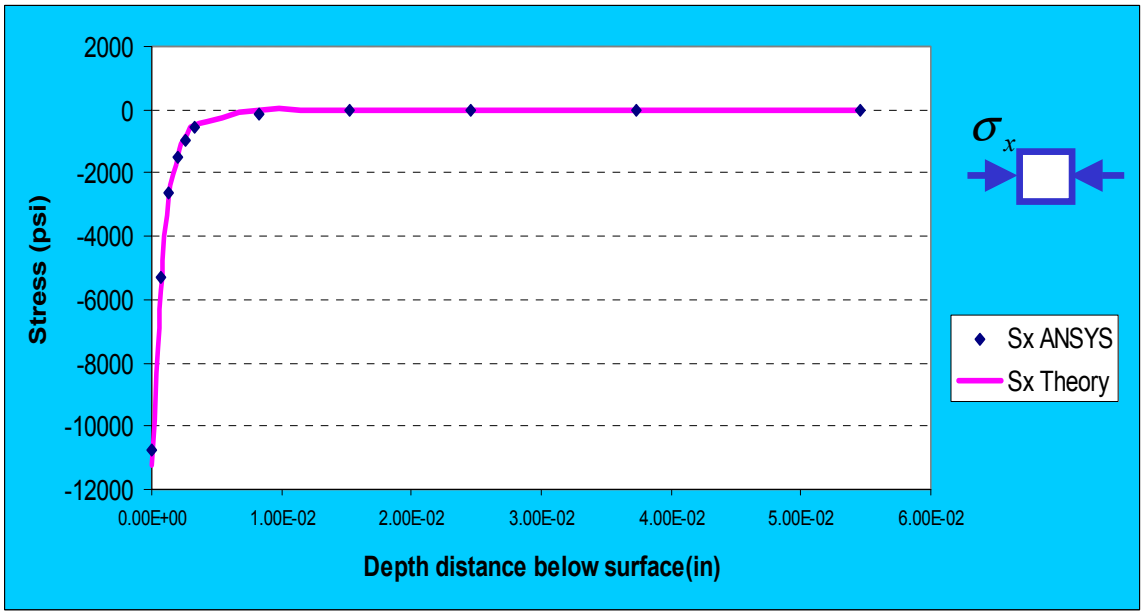


**Figure 3-9 FEM stresses agree with the theoretical values**

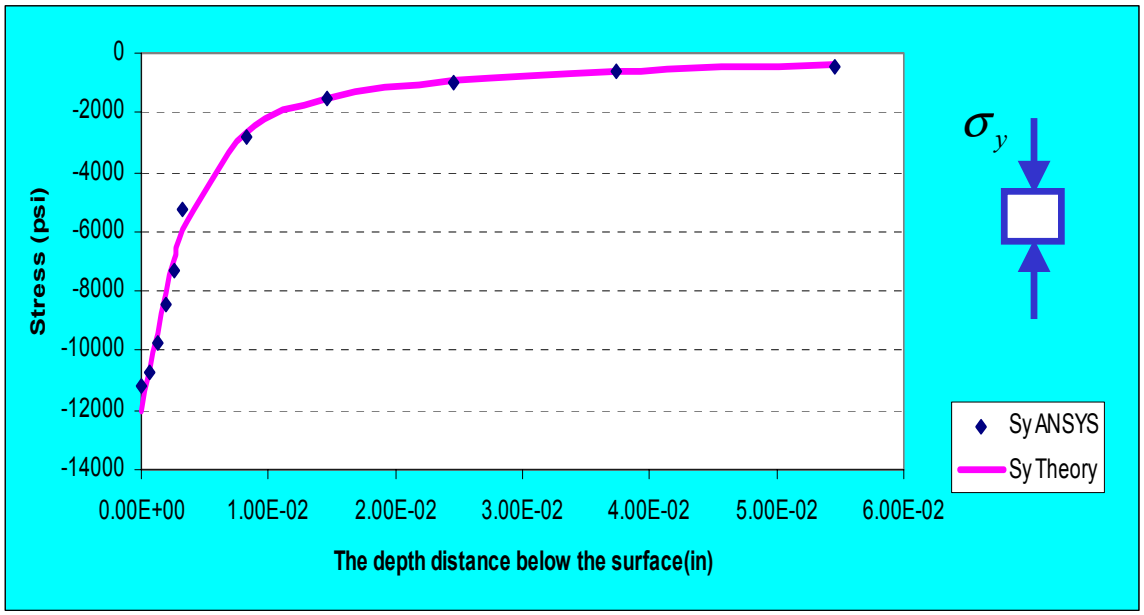


**Figure 3-10 Comparison between calculated values and ANSYS values**

Note that these above equations cannot be used to calculate the stresses on the surface because if we set y equal zero it will result in the stresses being calculated as zero. The peak values of the equivalent stress using the Von Mises criterion, the maximum shear stress, and the maximum orthogonal shear stress can be calculated from the maximum Hertz stress (3.7) as follows[1]:

$$\begin{aligned} \sigma_{VonMiss} &= 0.57\sigma_H, \\ \tau_{MaxShear} &= 0.30\sigma_H, \\ \tau_{OrthoShear} &= 0.25\sigma_H, \end{aligned} \tag{3.14}$$

where $\sigma_H$ is the maximum Hertz stress.

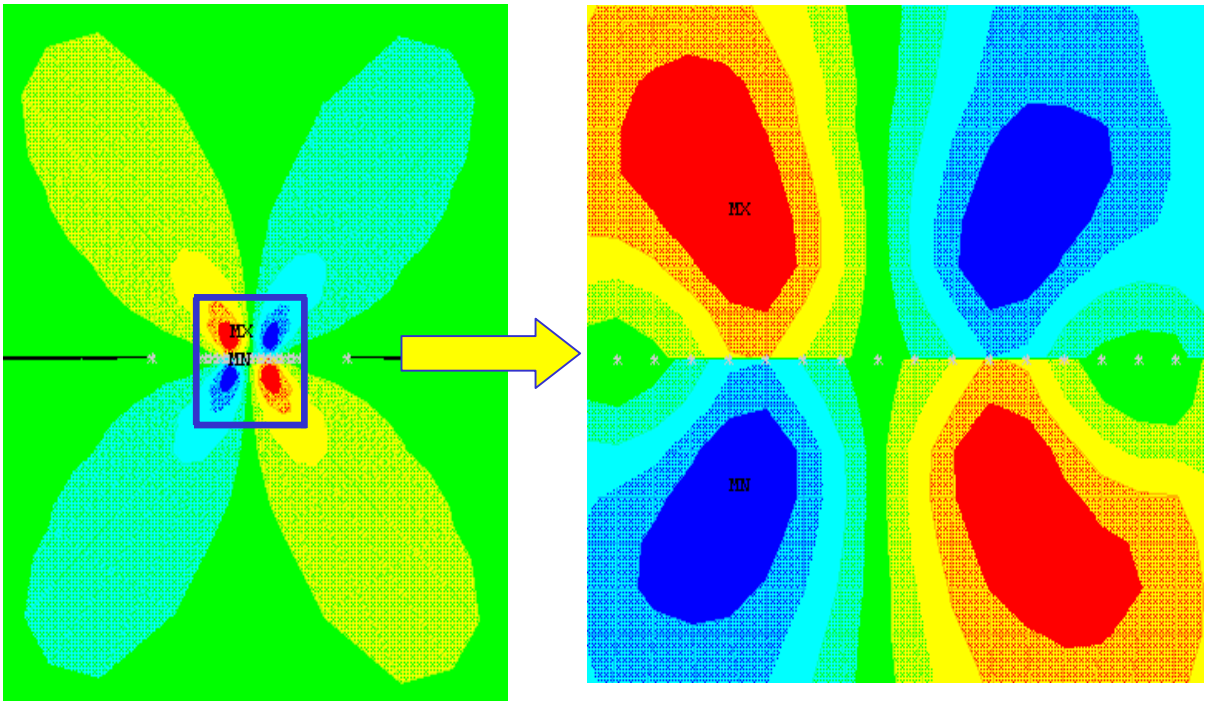


(*a*) (*b*)

**Figure 3-11 Orthogonal shear stress magnitudes**

Figure 3.9 and Figure 3.10 show a comparison of ANSYS results with the theoretical equations for stresses in x and y direction respectively. In both figures, the red curves represent the values from the above theoretical formula and blue points represent the results from ANSYS. It can be seen that the FEM results are essentially identical to the theoretical solution for both stresses $\sigma_x$ and $\sigma_y$. The FEA model from ANSYS is reliable if the solution is convergent. When finishing running the program, whether the solution has converged is checked after many times of equilibrium iteration. Usually a converged solution occurred at an expected "time" value such as the end of the load step.

If there is no convergence indicated in ANSYS, troubleshooting is necessary. Usually for nonlinear problems it is not easy to get convergence. In the author's experience, there are several ways to do that: (1) Change the FKN – Normal Penalty Stiffness value (2) Solve the nonlinear analysis using "Line Search", which can provide rapid convergence (3) Increasing the number of sub-steps. As long as the solution has converged, one can get a great deal of information from "General Postproc" for example : Von Mises, Principal, Shear, Contact Stresses.

Figures 3.11 (a) and (b) show orthogonal shear stress. Figures 3.12 (a) and (b) show maximum shear stresses under the contact areas between two cylinders. The largest orthogonal shear stress lies below the surface at the edge of the contact zone. This was shown in Figure 3.11 (b). The subsurface location of the maximum shear stress can also be seen lying below the surface at the center of the contact zone shown in Figure 3.12 (b). If both materials are steel, it occurs at a depth of about $0.63a$ where a is half of the contact length shown in Figure 3.4 and its magnitude is about $0.30P_{\max}$. The shear stress is about $0.11P_{\max}$ at the surface on the $z$ axis. The subsurface location of the maximum

shear stress is believed to be a significant factor in surface-fatigue failure. The theory indicates that cracks that begin below the surface eventually grow to the point that the material above the crack breaks out to form a pit.

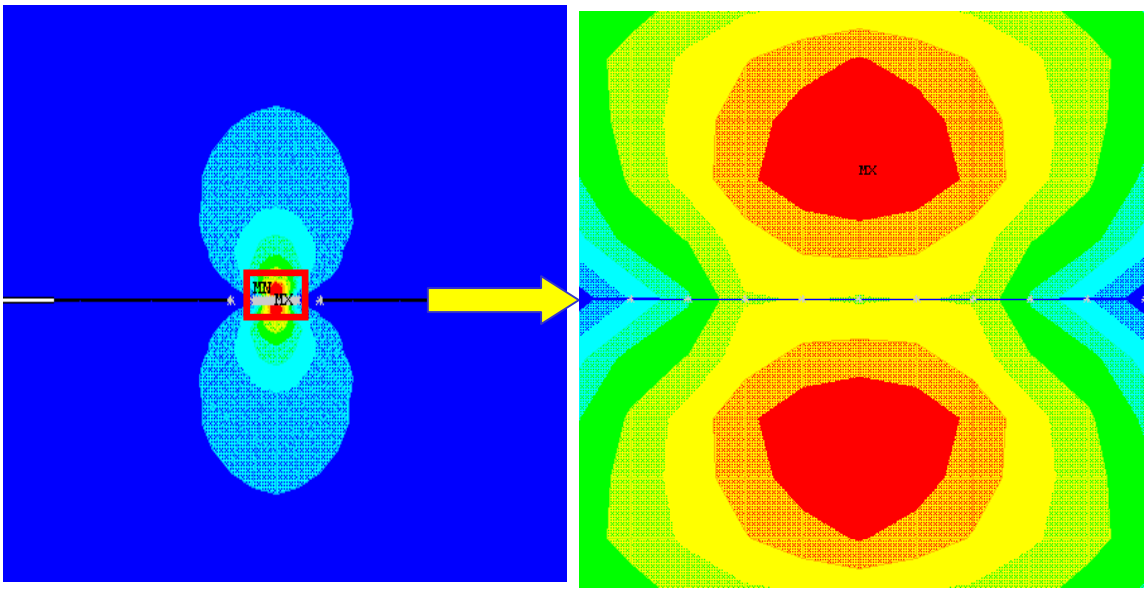


(*a*) (*b*)

**Figure 3-12 Maximum shear stress from ANSYS**

### 3.5 Conclusion

Finite element modelling of the contact between two cylinders was examined in detail. The finite element method with special techniques, such as the incremental technique of applying the external load in the input file, the deformation of the stiffness matrix, and the introduction of the contact element were used. It was found that initial loading using displacements as inputs was helpful in reducing numerical instabilities.

# Chapter 4 Involute Gear Tooth Contact and Bending Stress Analysis

## 4.1 Introduction

When one investigates actual gears in service, the conditions of the surface and bending failure are two of the most important features to be considered. The finite element method is very often used to analyze the stress states of elastic bodies with complicated geometries, such as gears. There are published papers, which have calculated the elastic stress distributions in gears. In these works, various calculation methods for the analysis of elastic contact problems have been presented. The finite element method for two-dimensional analysis is used very often. It is essential to use a three-dimensional analysis if gear pairs are under partial and nonuniform contact. However, in the three-dimensional calculation, a problem is created due to the large computer memory space that is necessary. In this chapter to get the gear contact stress a 2-D model was used. Because it is a nonlinear problem it is better to keep the number of nodes and elements as low as possible. In the bending stress analysis the 3-D model and 2-D models are used for simulation.

## 4.2 Analytical Procedure

From the results obtained in chapter 3 the present method is an effective and accurate method, which is proposed to estimate the tooth contact stresses of a gear pair. Special techniques of the finite element method were used to solve contact problems in chapter 3. Using the present method, the tooth contact stresses and the tooth deflections of a pair of spur gears analyzed by ANSYS 7.1 are given in section 4.4. Since the present

method is a general one, it is applicable to many types of gears. In early works, the following conditions were assumed in advance:

- There is no sliding in the contact zone between the two bodies
- The contact surface is continuous and smooth

Using the present method ANSYS can solve the contact problem and not be limited by the above two conditions. A two-dimensional and an asymmetric contact model were built. First, parameter definitions were given and then many points of the involute profile of the pinion and gear were calculated to plot an involute profile using a cylindrical system. The equations of an involute curve below were taken from Buckingham [6]:

$$\begin{aligned} r &= r_b * (1+\beta^2)^{1/2} \\ \psi &= \theta + \frac{\pi}{2n_1} - \xi \\ \theta &= \tan\phi - \phi = inv\phi \end{aligned} \tag{4.1}$$

where $r$ = radius to the involute form, $r_b$ = radius of the base circle

$\beta = \xi + \phi$

$\theta$ = vectorial angle at the pitch circle

$\xi$ = vectorial angle at the top of the tooth

$\phi$ = pressure angle at the pitch circle

$\phi_1$ = pressure angle at radius $r$

One spur tooth profile was created using equation 4.1, shown in Figure 4.1, as are the outside diameter circle, the dedendum circle, and base circle of the gear.

Secondly, in ANSYS from the tool bars using “CREATE”, “COPY”, “MOVE”, and “MESH” and so on, any number of teeth can be created and then kept as the pair of gear teeth in contact along the line of the action. The contact conditions of gear teeth are sensitive to the geometry of the contacting surfaces, which means that the element near the contact zone needs to be refined. It is not recommended to have a fine mesh everywhere in the model, in order to reduce the computational requirements. There are two ways to build the fine mesh near the contact surfaces. One is the same method as presented in chapter 3, a fine mesh of rectangular shapes were constructed only in the contact areas. The other one, “SMART SIZE” in ANSYS, was chosen and the fine mesh near the contact area was automatically created. A FEM gear contact model was generated as shown in Figure 4.2.

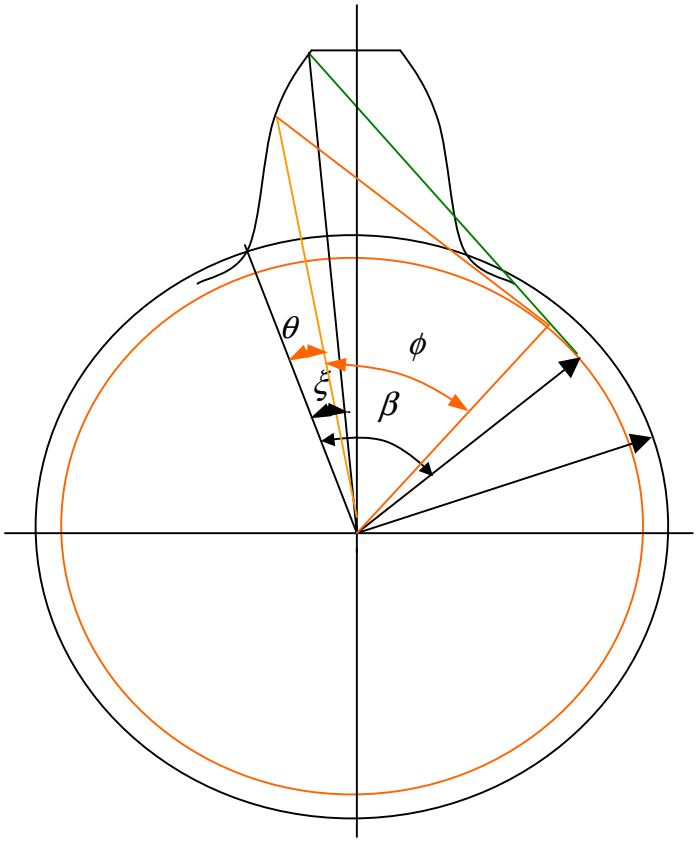


**Figure 4-1 Involutometry of a spur gear**

Thirdly, proper constraints on the nodes were given. The contact pair was inserted between the involute profiles, the external loads were applied on the model from ANSYS "SOLUTION > DEFINE LOAD > FORCE / MOMENT", and finally, ANSYS was run to get the solution.

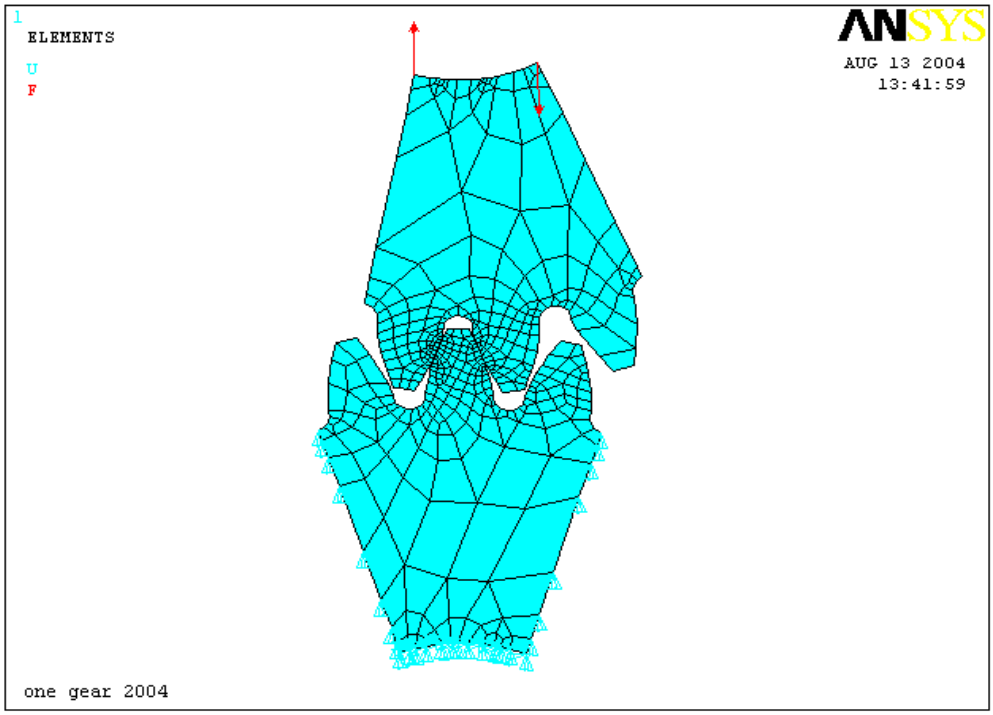


**Figure 4-2 Gear contact stress model**

## 4.3 Rotation Compatibility of the Gear Body

In order to know how much load is applied on the contact stress model and the bending stress model, evaluating load sharing between meshing gears is necessary. It is also an important concept for transmission error. It is a complex process when more than one-tooth pair is simultaneously in contact taking into account the composite tooth deflections due to bending, shearing and contact deformation. This section presents a

general approach as to how the load is shared between the meshing teeth in spur gear pairs.

When the gears are put into mesh, the line tangent to both base circles is defined as the line of action for involute gears. In one complete tooth mesh circle, the contact starts at points A shown in Figure 4.3 [64] where the outside diameter circle, the addendum circle of the gear intersects the line of action. The mesh cycle ends at point E, as shown in Figure 4.4 where the outside diameter of the pinion intersects the line of action.

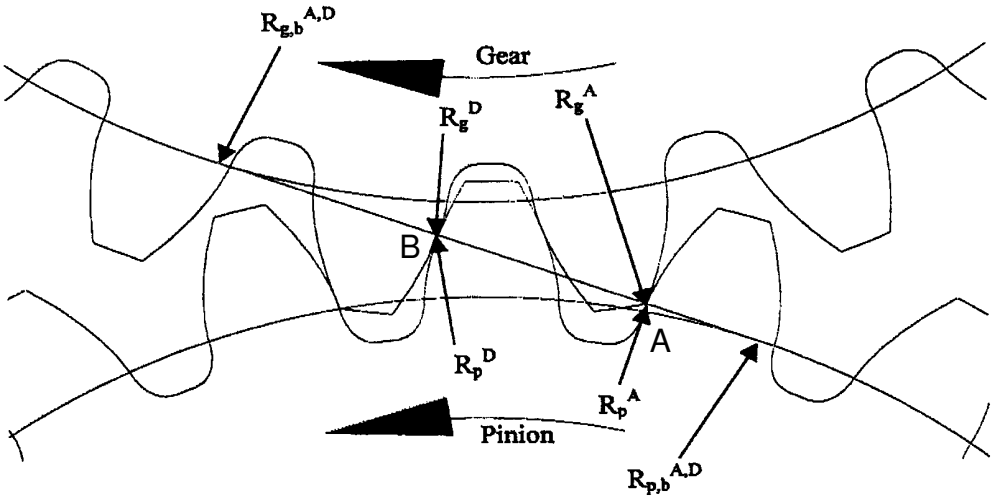


**Figure 4-3 Illustration of one complete tooth meshing cycle**

Consider two identical spur gears in mesh. When the first tooth pair is in contact at point A it is between the tooth tip of the output gear and the tooth root of the input gear (pinion). At the same time a second tooth pair is already in contact at point D in Figure

4.3. As the gear rotates, the point of contact will move along the line of action APE. When the first tooth pair reaches point B shown in Figure 4.4, the second tooth pair disengage at point E leaving only the first tooth pair in the single contact zone. After this time there is one pair of gear in contact until the third tooth pair achives in contact at point A again. When this tooth pair rotates to point D, the another tooth pair begins engagement at point A which starts another mesh cycle. After this time there are two pairs of gear in contact until the first tooth pair disengage at point E. Finally, one complete tooth meshing cycle is completed when this tooth pair rotates to point E. To simplify the complexity of the problem, the load sharing compatibility condition is based on the assumption that the sum of the torque contributions of each meshing tooth pair must equal the total applied torque.

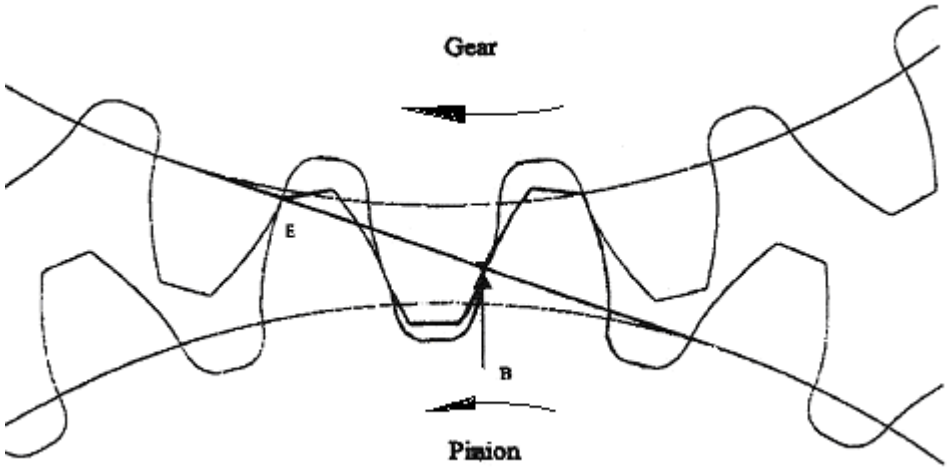


**Figure 4-4 Different positions for one complete tooth meshing cycle**

Analytical equations can also be developed for the rotation of the gear and pinion hubs, including the effects of tooth bending deflection and shearing displacement and

contact deformation [64]. In the pinion reference frame, it is assumed that the pinion hub remains stationary, while the gear rotates due to an applied torque.

Considering the single pair contact zone at point B, the condition of angular rotation of the gear body will then be given by [64]

For the pinion,
$$\theta_P^B = \frac{B_P^B + H_P^B}{R_P^B} \tag{4.2}$$

and for the gear,
$$\theta_g^B = \frac{B_g^B + H_g^B}{R_g^B} \tag{4.3}$$

where $B_P^B$ and $B_g^B$ are the tooth displacement vectors caused by bending and shearing for pairs B of the pinion and gear respectively, $H_P^B$ and $H_g^B$ are the contact deformation vectors of tooth pair B of the pinion and gear respectively. $\theta_P^B$ denotes the transverse plane angular rotation of the pinion body caused by bending deflection, shearing displacement and contact deformation of the tooth pair B while the gear is stationary. Conversely, for the gear rotation while the pinion is stationary, $\theta_g^B$ gives the transverse plane angular rotations of the gear body.

## 4.4 Gear Contact Stress

One of the predominant modes of gear tooth failure is pitting. Pitting is a surface fatigue failure due to many repetitions of high contact stress occurring on the gear tooth surface while a pair of teeth is transmitting power. In other words, contact stress exceeding surface endurance strength with no endurance limits or a finite life causes this kind of failure. The AGMA has prediction methods in common use. Contact failure in gears is currently predicted by comparing the calculated Hertz stress to experimentally-determined allowable values for the given material. The details of the subsurface stress

field usually are ignored. This approach is used because the contact stress field is complex and its interaction with subsurface discontinuities are difficult to predict. However, all of this information can be obtained from the ANSYS model.

Since a spur gear can be considered as a two-dimensional component, without loss of generality, a plane strain analysis can be used. The nodes in the model were used for the analysis. The nodes on the bottom surface of the gear were fixed. A total load is applied on the model. It was assumed to act on the two points shown in Figure 4.2 and three points in Figure 4.5.

There are two ways to get the contact stress from ANSYS. Figure 4.5 shows the first one, which is the same method as one in chapter 3 to create the contact element COCNTA 48 and the rectangular shape fine mesh beneath the contact surfaces between the contact areas. Figure 4.6 shows the enlarged-area with a fine mesh which is composed of rectangular shapes.

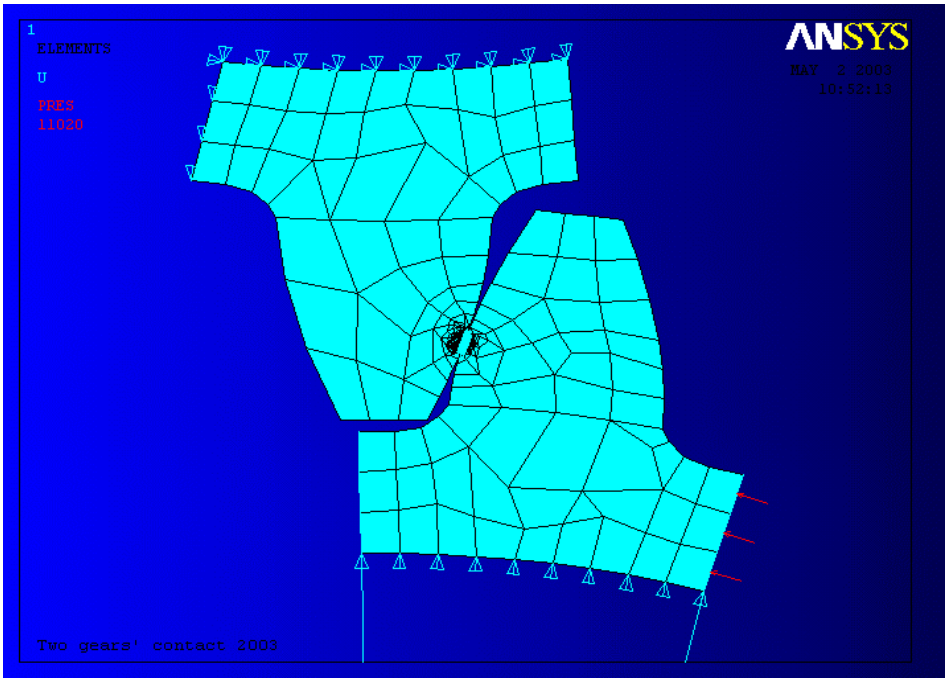


**Figure 4-5 FEM Model of the gear tooth pair in contact**

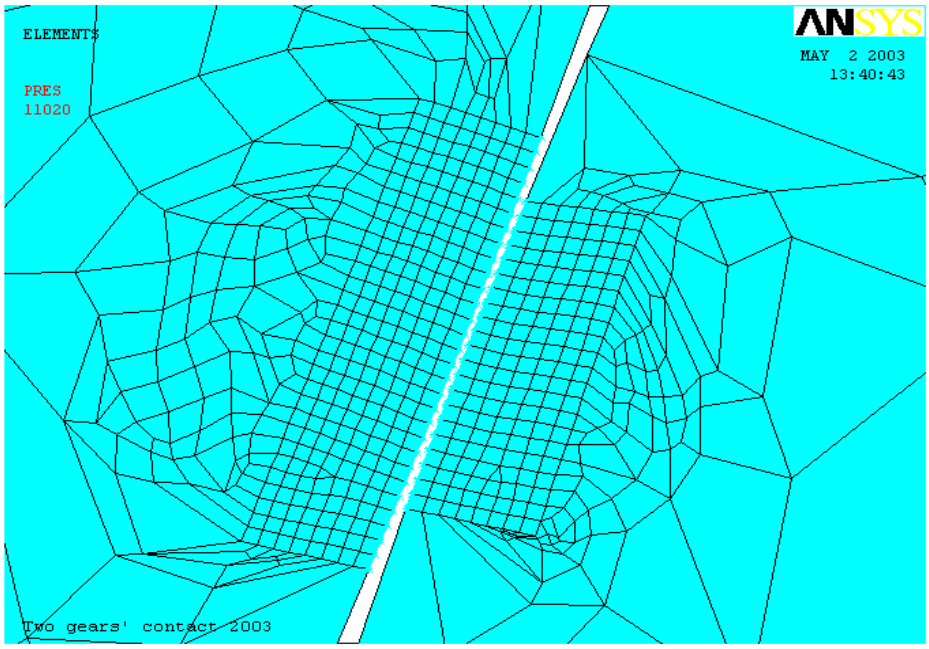


**Figure 4-6 Fine meshing of contact areas**

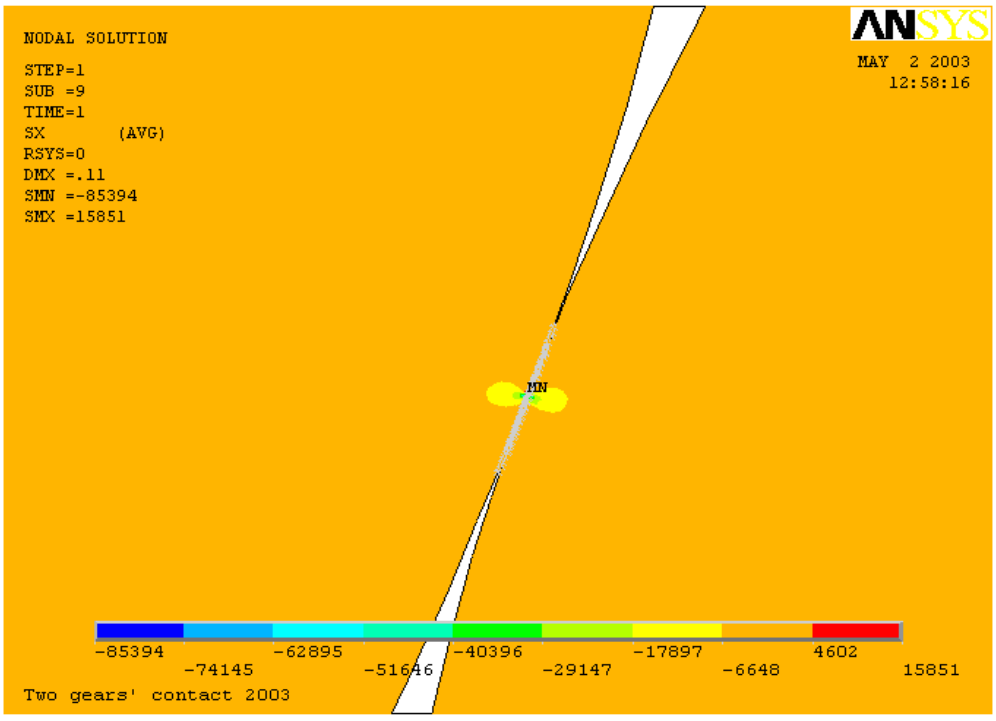


**Figure 4-7 Contact stress along contact areas**

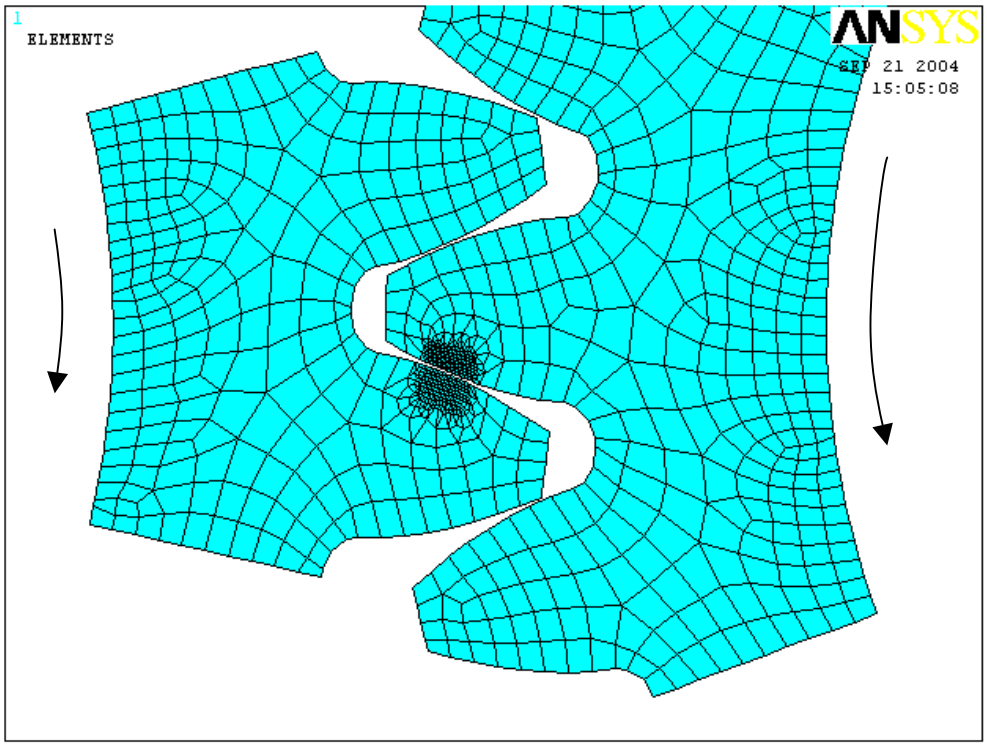


**Figure 4-8 A fine mesh near contact areas**

Figure 4.7 shows the normal contact stress along the contact areas. The results are very similar to the results in the two cylinders in chapter 3. Figure 4.8 presents how to mesh using a second method. Different methods should show the close results of maximum contact stress if the same dimension of model and the same external loads are applied on the model. If there is a small difference it is likely because of the different mesh patterns and restricted conditions in the finite element analysis and the assumed distribution form of the contact stresses in the contact zone.

## 4.5 The Lewis Formula

There are several failure mechanisms for spur gears. Bending failure and pitting of the teeth are the two main failure modes in a transmission gearbox. Pitting of the teeth

is usually called a surface failure. This was already discussed in the last section. The bending stresses in a spur gear are another interesting problem. When loads are too large, bending failure will occur. Bending failure in gears is predicted by comparing the calculated bending stress to experimentally-determined allowable fatigue values for the given material. This bending stress equation was derived from the Lewis formula. Wilfred Lewis (1892) [5] was the first person to give the formula for bending stress in gear teeth using the bending of a cantilevered beam to simulate stresses acting on a gear tooth shown in Figure 4.9 are Cross-section $= b * t$, length = l, load $= F_t$, uniform across the face. For a rectangular section, the area moment of inertia is $I = \frac{bh^3}{12}$

$M = F_t l$ and $c = t/2$, stress then is

$$\sigma = \frac{M}{I/c} = \frac{F_t l(t/2)}{bt^3/12} = \frac{6F_t l}{bt^2} \tag{4.4}$$

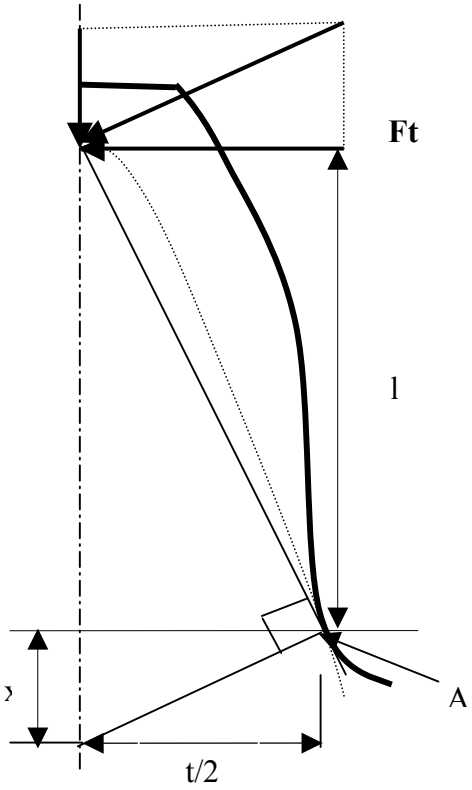


**Figure 4-9 Length dimensions used in determining bending tooth stress**

Where $b =$ the face width of the gear. For a gear tooth, the maximum stress is expected at point A, which is a tangential point where the parabola curve is tangent to the curve of the tooth root fillet called parabola tangential method. Two points can be found at each side of the tooth root fillet. The stress on the area connecting those two points is thought to be the worst case. The crack will likely start from the point A.

From similar triangles $\tan\alpha = \frac{t/2}{x} = \frac{l}{t/2}$ where $l = \frac{t^2}{4x}$ (4.5)

Substituting (4.7) into (4.6):

$$\sigma = \frac{6F_t \frac{t^2}{4x}}{bt^2} = \frac{3F_t}{2bx} = \frac{3F_t p_d}{2bp_d x} = \frac{F_t p_d}{bY} \quad (4.6)$$

where $p_d =$ diametral pitch

$$Y = \frac{2}{3}\frac{xp_d}{} = \text{Lewis form factor} \quad (4.7)$$

Equation (4.8) [5] in the next page is known as the Lewis equation, and $Y$ is called the Lewis form factor. The Lewis equation considers only static loading and does not take the dynamics of meshing teeth into account. The Lewis form factor is given for various numbers of teeth while assuming a pressure angle of $20^\circ$ and a full – depth involute. The Lewis form factor is dimensionless, and is also independent of tooth size and only a function of shape. The above stress formula must be modified to account for the stress concentration $K_c$. The concentrated stress on the tooth fillet is taken into account by $K_c$ and a geometry factor $Y_j$, where $Y_j = Y / K_c$ is introduced. Other modifications are recommended by the AGMA for practical design to account for the variety of conditions that can be encountered in service. The following design equation, developed by Mott (1992) is used

$$\sigma_t = \frac{F_t p_d K_a K_s K_m}{b Y_j K_v} \tag{4.8}$$

where $K_a$ = application factor , $K_s$ = size factor ,

$K_m$ = load distribution factor, $K_v$ = dynamic factor,

$F_t$ = normal tangential load, $Y_j$ = Geometry factor.

Each of these factors can be obtained from the books on machine design such as [5]. This analysis considers only the component of the tangential force acting on the tooth, and does not consider effects of the radial force, which will cause a compressive stress over the cross section on the root of the tooth. Suppose that the greatest stress occurs when the force is exerted at top of tooth, which is the worst case. When the load is at top of the tooth, usually there are a least two tooth pairs in contact. In fact, the maximum stress at the root of tooth occurs when the contact point moves near the pitch circle because there is only one tooth pair in contact and this teeth pairs carries the entire torque. When the load is moving at the top of the tooth, two teeth pairs share the whole load if the ratio is larger than one and less than two. If one tooth pair was considered to carry the whole load and it acts on the top of the tooth this is adequate for gear bending stress fatigue.

## 4.6 FEM Models

### 4.6.1 The Two Dimensional Model

Fatigue or yielding of a gear tooth due to excessive bending stresses are two important gear design considerations. In order to predict fatigue and yielding, the maximum stresses on the tensile and compressive sides of the tooth, respectively, are required. In the past, the bending stress sensitivity of a gear tooth has been calculated using photo elasticity or relatively coarse FEM meshes. However, with present computer

developments we can make significant improvements for more accurate FEM simulations.

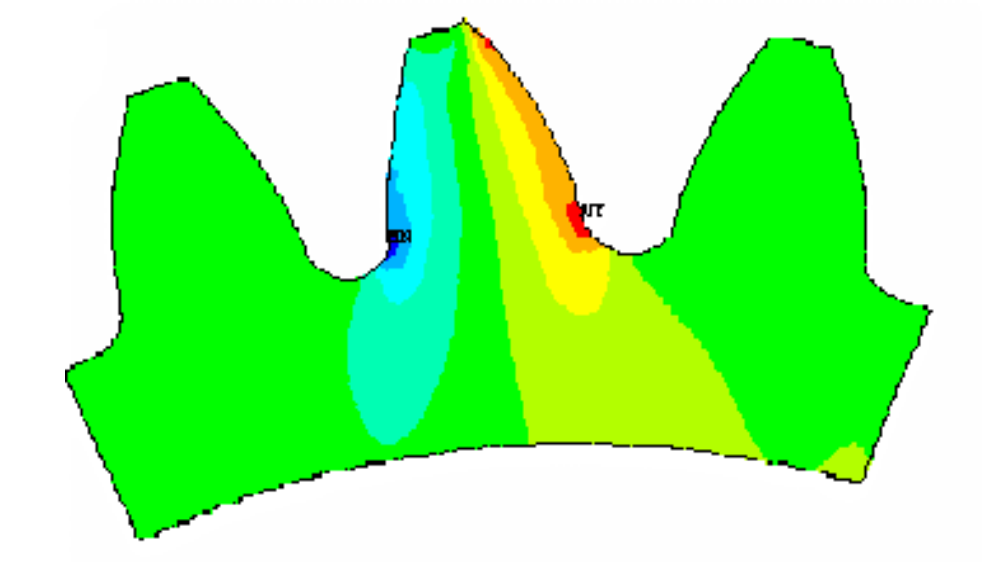

**Figure 4-10 FEM gear tooth bending model with 3 teeth**

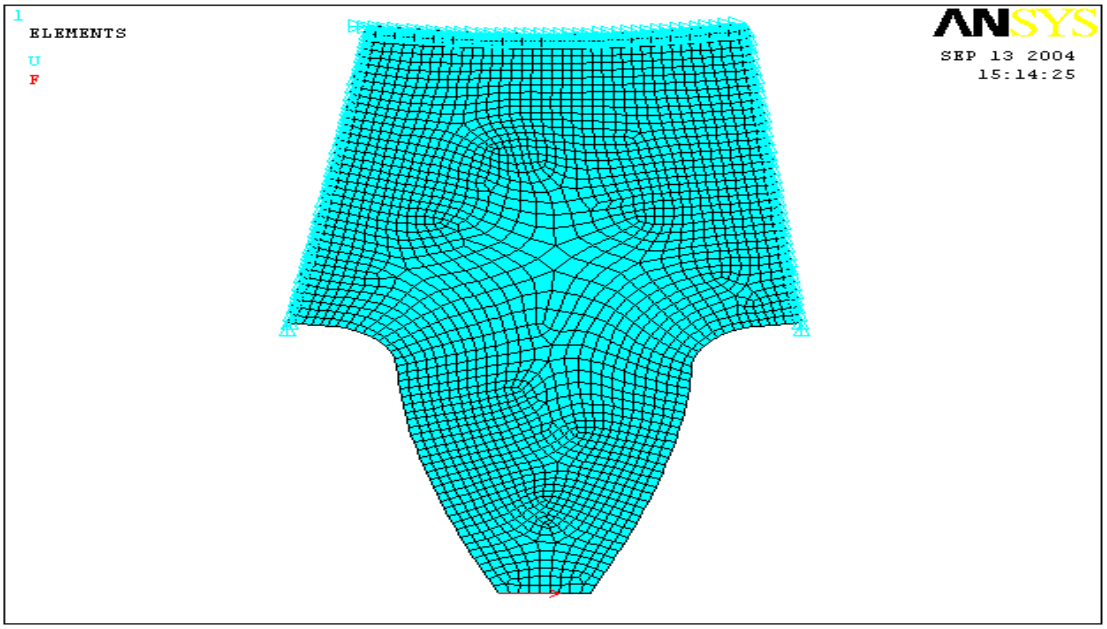


**Figure 4-11 A two dimension tooth from a FEM model with 28 teeth**

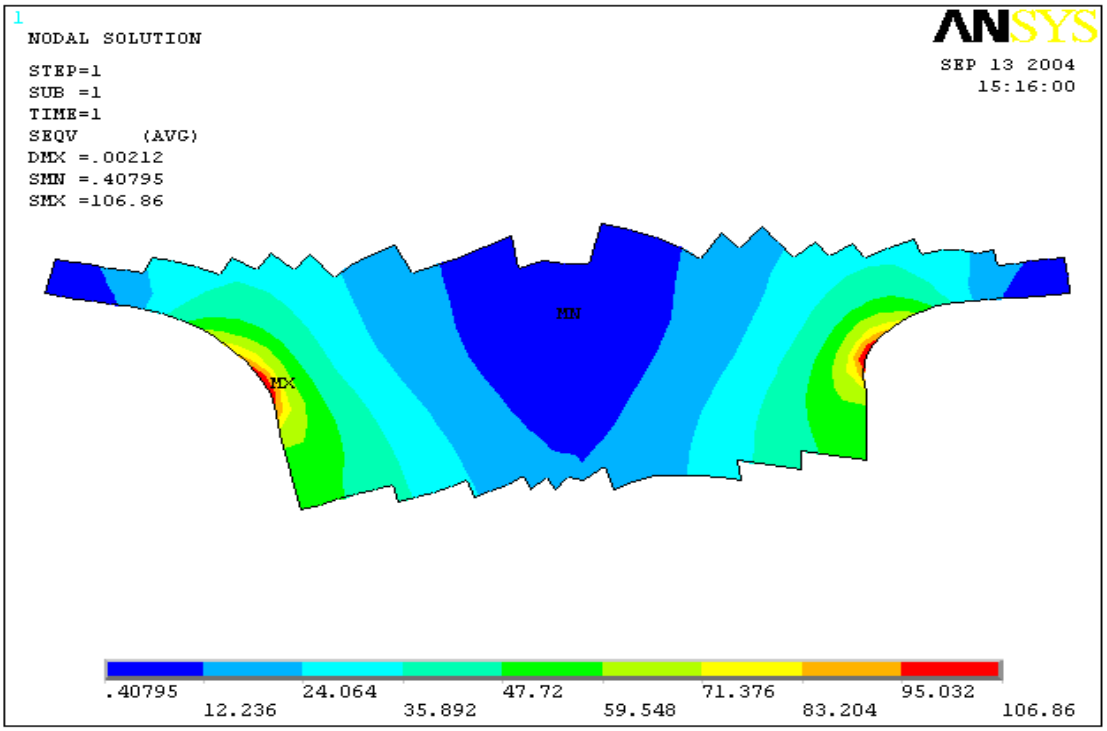


**Figure 4-12 Von Mises stresses with 28 teeth on the root of tooth**

In the procedure for generating a FEM model for bending stress analyses, the equations used to generate the gear tooth profile curve were the same as the ones in section 4.2. When meshing the teeth in ANSYS, if "SMART SIZE" is used the number of elements near the roots of the teeth are automatically much greater than in other places. Figure 4.10 shows that the maximum tensile stresses on the tensile side and maximum compressive stresses on other side of the tooth, respectively. It also indicates that only one tooth is enough for the bending stress analysis for the 3-D model or the 2-D model. Figure 4.11 shows one tooth FEM model and Figure 4.12 shows how much Von Mises stress is on the root of tooth when the number of teeth is 28 for the gear. There are more detailed results for different number of teeth in table 4.1 in section 4.7, which are compared with the results from the Lewis Formula.

### 4.6.2 The Three Dimensional Model

In this section the tooth root stresses and the tooth deflection of one tooth of a spur gear is calculated using an ANSYS model. For the bending stresses, the numerical results are compared with the values given by the draft proposal of the standards of the AGMA in the next section.

Figure 4.14 shows how to mesh the 3D model and how to apply the load on the model. The element type "SOLID TETRAHEDRAL 10 NODES 187" was chosen. Because "SMART SET" was chosen on the tool bar there are many more elements near the root of the tooth than in other places. There are middle side nodes on the each side of each element. So a large number of degrees of freedom in this 3D model take a longer time to finish running.

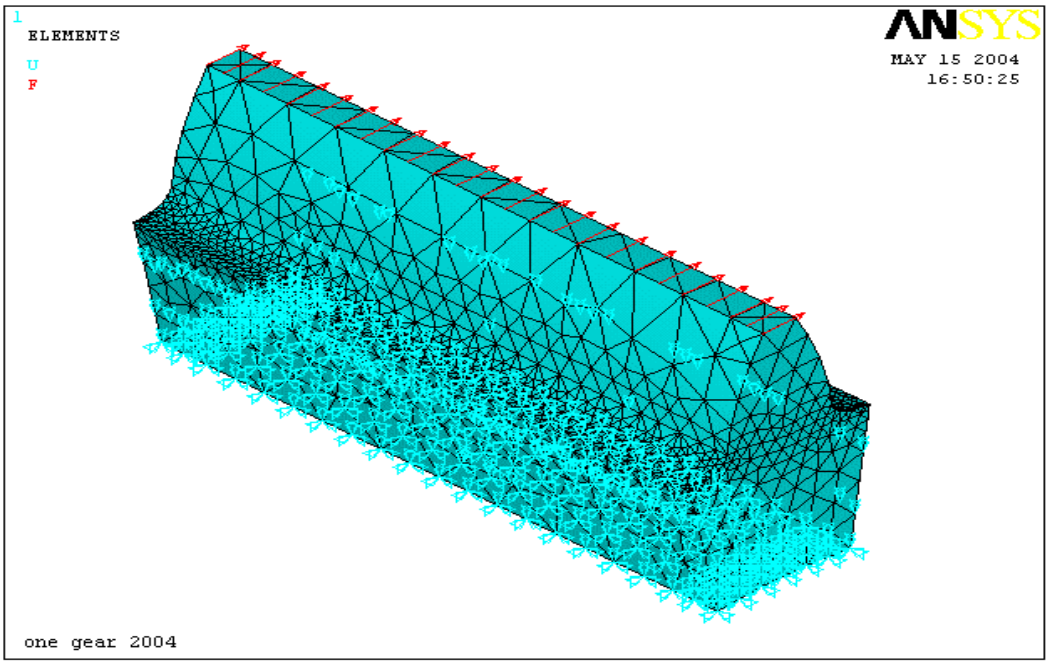


**Figure 4-13 FEM bending model with meshing**

From the stress distributions on the model, the large concentrated stresses are at the root of the tooth. Figure 4.14 shows large Von Mises stresses at the root of the tooth. They are equal to the tensile stresses. The tensile stresses are the main cause of crack failure, if they are large enough. That is why cracks usually start from the tensile side. From the Lewis equation if the diameters of the pinion and gear are always kept the same and the number of teeth was changed, the diametral pitch will be changed or the module of gear will be changed. That means that there are different bending strengths between the different teeth numbers. Different Maximum Von Mises with different numbers of teeth are shown in the table 4.1.

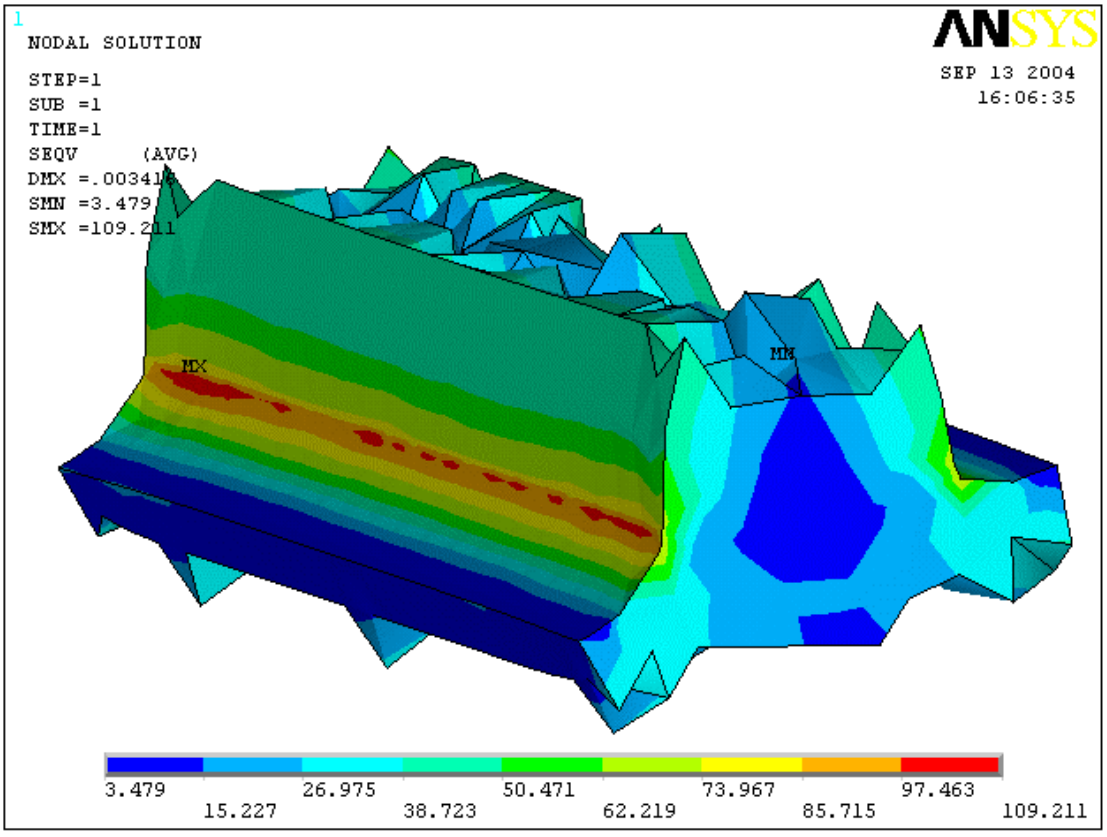


**Figure 4-14 Von Mises stresses with 28 teeth on the root of tooth**

## 4.7 Comparison with Results using AGMA Analyses

In this section, a comparison of the tooth root stresses obtained in the three dimensional model and in the two dimensional model using ANSYS with the results given by the standards of the AGMA is carried out. Eq. (4.8) is recommended by the AGMA and the other coefficients, such as the dynamic factor, are set at 1.2. Here analysis of gears with different numbers of teeth are carried out. First, the number of gear teeth is 28. The meshing spur gear has a pitch radii of 50 mm and a pressure angle of $20^{\circ}$. The gear face width, b = 1.5 in (38.1mm). The transmitted load is 2500 N.

$$50mm = 1.9685in \qquad 2500N = 562.02Pounds$$

$$p_d = \frac{N}{d} = \frac{28}{1.9685 * 2} = 7.112$$

$$\sigma_t = \frac{F_t p_d K_a K_s K_m}{b Y_j K_v} = \frac{562.022 * 7.112 * 1.2 * 1.2 * 1.15}{1.5 * 0.37 * 0.8} = 102.783MPa$$

Detailed investigations, including the effects with the two different numbers of teeth on the tooth root stress were carried out. If the number of teeth is changed from 28 to 23 and the other parameters were kept the same.

$$\sigma_t = \frac{F_t p_d K_a K_s K_m}{b Y_j K_v} = \frac{562.022 * 5.842 * 1.2 * 1.2 * 1.15}{1.5 * 0.37 * 0.8} = 84.429MPa$$

If the number of teeth is changed from 28 to 25 and the other parameters were kept the same.

$$\sigma_t = \frac{F_t p_d K_a K_s K_m}{b Y_j K_v} = \frac{562.022 * 6.35 * 1.2 * 1.2 * 1.15}{1.5 * 0.37 * 0.8} = 91.770MPa$$

If the number of teeth is changed from 28 to 34 with the other parameters kept the same.

$$\sigma_t = \frac{F_t p_d K_a K_s K_m}{b Y_j K_v} = \frac{562.022 * 8.636 * 1 * 1 * 1.15}{1.5 * 0.37 * 0.8} = 124.805 MPa$$

If the number of teeth is changed to 37, with the other parameters kept the same.

$$\sigma_t = \frac{F_t p_d K_a K_s K_m}{b Y_j K_v} = \frac{562.022 * 9.398 * 1 * 1 * 1.15}{1.5 * 0.37 * 0.8} = 132.149 MPa$$

The above calculations of the Von Mises stresses on the root of tooth were carried out in order to know if they match the results from ANSYS. The results are shown in Table 4.1. In this table, the maximum values of the tooth root stress obtained by the ANSYS method were given. For the number of teeth of 28, the ANSYS results are about 97% (2D) of the values obtained by the AGMA. For the cases from 23 teeth to 37 teeth, the values range from 91% to 99% of the value obtained by the AGMA. From these results, it was found that for all cases give a close approximation of the value obtained by the methods of the AGMA in both 3D and 2D models. These differences are believed to be caused by factors such as the mesh pattern and the restricted conditions on the finite element analysis, and the assumed position of the critical section in the standards.

Here the gears are taken as a plane strain problem. 2D models are suggested to be use because much more time will be saved when running the 2D models in ANSYS. There are not great differences between the 3D and 2D model in Table 4.1.

**Table 4.1 Von Mises Stress of 3-D and 2-D FEM bending model**

| Num.of teeth | Stress 3D (2D) (ANSYS) | Stresses (AGMA) | Difference 3D (2D) |
|---|---|---|---|
| 23 | 86.418 (85.050) | 84.429 | 2.35% (0.74%) |
| 25 | 95.802 (91.129) | 91.770 | 4.39% (0.69%) |
| 28 | 109.21 (106.86) | 102.78 | 6.26% (3.97%) |
| 31 | 123.34 (116.86) | 113.79 | 8.39% (2.69%) |
| 34 | 132.06 (128.46) | 124.80 | 5.82% (2.93%) |
| 37 | 143.90 (141.97) | 132.15 | 8.89% (7.43%) |

## 4.8 Conclusion

In the present study, effective methods to estimate the tooth contact stress by the two-dimensional and the root bending stresses by the three-dimensional and two-dimensional finite element method are proposed. To determine the accuracy of the present method for the bending stresses, both three dimensional and two dimensional models were built in this chapter. The results with the different numbers of teeth were used in the comparison. The errors in the Table 4.1 presented are much smaller than previous work done by other researchers for the each case. So those FEA models are good enough for stress analysis.

# Chapter 5 Torsional Mesh stiffness and Static Transmission Error

## 5.1 Introduction and Definition of Transmission Error

Getting and predicting the static transmission error (TE) is a necessary condition for reduction of the noise radiated from the gearbox. In the previous literature to obtain TE the contact problem was seldom included because the nonlinear problem made the model too complicated. This chapter deals with estimation of static transmission error including the contact problem and the mesh stiffness variations of spur gears. For this purpose, an FEA numerical modeling system has been developed. For spur gears a two dimensional model can be used instead of a three dimensional model to reduce the total number of the elements and the total number of the nodes in order to save computer memory. This is based on a two dimensional finite element analysis of tooth deflections. Two models were adopted to obtain a more accurate static transmission error, for a set of successive positions of the driving gear and driven gear. Two different models of a generic gear pair have been built to analyze the effects of gear body deformation and the interactions between adjacent loaded teeth. Results are from each of the two models' average values.

It is generally accepted that the noise generated by a pair of gears is mainly related to the gear transmission error. The main source of apparent excitation in gearboxes is created by the meshing process. Researchers usually assume that transmission error and the variation in gear mesh stiffnesses are responsible for the noise radiated by the gearbox. The static transmission error is defined by Smith [59].

The term transmission error is used to describe the difference between the theoretical and actual relative angular rotations between a pinion and a gear. Its characteristics depend on the instantaneous positions of the meshing tooth pairs. Under load at low speeds (static transmission error) these situations result from tooth deflections and manufacturing errors. In service, the transmission error is mainly caused by:

- Tooth geometry errors: including profile, spacing and runout errors from the manufacturing process;
- Elastic deformation: local contact deformation from each meshing tooth pair and the deflections of teeth because of bending and shearing due to the transmitted load;
- Imperfect mounting: geometric errors in alignment, which may be introduced by static and dynamic elastic deflections in the supporting bearings and shafts.

The first two types of transmission errors are commonly referred to in the literature [7][17]. The first case has manufacturing errors such as profile inaccuracies, spacing errors, and gear tooth runout. When the gears are unloaded, a pinion and gear have zero transmission error if there is no manufacturing error. The second case is loaded transmission error, which is similar in principle to the manufactured transmission error but takes into account tooth bending deflection, and shearing displacement and contact deformation due to load. In chapter 5 the second case is considered.

The static transmission error of gears in mesh at particular positions throughout the mesh cycle was generated in this study by rotating both solid gears one degree each time then creating a finite element model in that particular position. In order to develop representative results, a large number of finite element models at the different meshing positions were undertaken for this investigation. One of the most important criteria for each model was that the potential contact nodes of both surfaces would be created on the

nodes near the intersection point between the pressure line and the involute curve for that particular tooth. The additional problem of determining the penalty parameter at each contact position could be user-defined or a default value in the finite element model. At each particular meshing position, after running ANSYS the results for angular rotation of the gear due to tooth bending, shearing and contact displacement were calculated. In the pinion reference frame: the local cylindrical system number 12 was created by definition in ANSYS. By constraining the all nodes on the pinion in radius and rotating $\theta_g$ with the gear having a torque input load the model was built. In this case, $\theta_p = 0$ and $\theta_g$ is in the opposite direction to that resulting from forward motion of $\theta_p$ changing the TE result to positive as seen by equation (5.1)

$$TE = \theta_g - (Z)\theta_p \tag{5.1}$$

Where Z is the gear ratio and $\theta_{p,g}$ is the angular rotation of the input and output gears in radians respectively. In relation to the gear reference frame: the local cylindrical system number 11, the gear was restrained with degrees of freedom in radius and rotating $\theta_p$ with the pinion having the torque input load and the resulting angular rotation of the pinion was computed. In this second case $\theta_g = 0$ and the TE will be positive for forward motion of $\theta_g$. After compensating for torque and angular rotation for the particular gear ratio, the results from these two models should be the same, and so the mean of these two angular rotations would give the best estimate of the true static transmission error of the involute profile gears under load.

## 5.2 The Combined Torsional Mesh Stiffness

Because the number of the teeth in mesh varies with time, the combined torsional mesh stiffness varies periodically. When a gear with perfect involute profiles is loaded

the combined torsional mesh stiffness of the gear causes variations in angular rotation of the gear body. The gear transmission error is related directly to the deviation of the angular rotation of the two gear bodies and the relative angular rotation of the two gears is inversely proportional to the combined torsional mesh stiffness, which can be seen from the results of ANSYS later in this document. The combined torsional mesh stiffness is different throughout the period of meshing position. It decreases and increases dramatically as the meshing of the teeth change from the double pair to single pair of teeth in contact.

In other words under operating conditions, the mesh stiffness variations are due to variations in the length of contact line and tooth deflections. The excitation located at the mesh point generates dynamic mesh forces, which are transmitted to the housing through shafts and bearings. Noise radiated by the gearbox is closely related to the vibratory level of the housing.

Sirichai [60] has developed a finite element analysis and given a definition for torsional mesh stiffness of gear teeth in mesh. The combined torsional mesh stiffness is defined as the ratio between the torsional load and the angular rotation of the gear body. The development of a torsional mesh stiffness model of gears in mesh can be used to determine the transmission error throughout the mesh cycle.

The combined torsional mesh stiffness of gears is time dependent during involute action due to the change in the number of contact tooth pairs. Considering the combined torsional mesh stiffness for a single tooth pair contact zone, the single tooth torsional mesh stiffness of a single tooth pair in contact is defined as the ratio between the torsional mesh load (T) and the elastic angular rotation $(\theta)$ of the gear body. In the single tooth pair contact zone, as the pinion rotates, the single tooth torsional mesh stiffness of the

pinion, $K_P$ is decreasing while the single tooth torsional stiffness of the gear, $K_g$, is increasing. When the pinion rotates to the pitch point $P$, the single tooth torsional stiffness of both gears is equal because both of them were assumed to be identical spur gears with ratio 1:1 in order to make the analysis simple. The single tooth torsional mesh stiffness of the pinion and the gear are given by [64],

$$K_P^B = \frac{T_P^B}{\theta_P^B} \tag{5.2}$$

$$K_g^B = \frac{T_g^B}{\theta_g^B} \tag{5.3}$$

where $K_P^B$ and $K_g^B$ are the single tooth torsional mesh stiffness of the single tooth pairs at B of the pinion and gear respectively.

The torsional mesh stiffness can be related to the contact stiffness by considering the normal contact force operating along the line of action tangential to the base circles of the gears in mesh. The torsional mesh stiffness can be seen to be the ratio between the torque and the angular deflection. By considering the total normal contact force *F*, acting along the line of action, the torque T will be given by the force multiplied by the perpendicular distance (base circle radius $r_b$) $T = Fr_b$ if there is one pair gear on contact. The elastic angle of rotation $\theta$ of the gear body can then be calculated from related to the arc length c, by the base circle radius as $\theta = c / r_b$. The torsional mesh stiffness can then be given by

$$K_m = \frac{T}{\theta} = \frac{Fr_b}{c / r_b} = \frac{Fr_b^2}{c} \tag{5.4}$$

The tooth contact stiffness $K_{mb}$, can be seen to be the ratio of the normal contact force $F$ to the displacement along the line of action, which gives $K_{mb} = F / a$, where the length $a$ is equal to the arc $c$ length for a small angles $\theta$. The relationship between the linear contact stiffness and torsional mesh stiffness then becomes,

$$K_{mb} = \frac{K_m}{r_b^2} \tag{5.5}$$

The contact between the gears is a nonlinear problem. This cannot be put in the form of a linear differential equation if the problem is solved by the equations so here ANSYS was used to study this problem. In this chapter the program ANSYS 7.1 was used to help to solve this nonlinear problem. The gears were modeled using quadratic two dimensional elements and the contact effect was modeled using 2D surface-to-surface (line-to-line) general contact elements that can include elastic Coulomb frictional effects. The torsional mesh stiffness of gears in mesh at particular positions throughout the mesh cycle was generated by rotating both solid gears one degree each time, then creating a finite element model in that particular position. The torsional mesh stiffness $K_m$ in mesh was automatically considered, when the transmission error was obtained from the results of the FEA model. Figure 5.1 shows how to apply load and how to define the input torque by a set of beam elements (beam3) connected from the nodes on the internal cycle of rim to the center point of the pinion, while restraining all nodes on the internal circle of the output gear hub. The center node of pinion was constrained in the X and Y directions and it was kept the degree of freedom for rotation around the center of the pinion. The moment was applied on the center of the pinion.

After running ANSYS for the each particular position of the FEA model there were volumous results from the postprocessor. For example, the Von Mises stresses,

contact stresses and deformations in the X and Y directions can easily be gotten. The static transmission error and the torsional mesh stiffness were then automatically obtained from ANSYS in the postprocessor. The vectors of displacement in the global system at one particular meshing position were shown in Figure 5.2. In Figure 5.2 $\theta$ represents TE at one position. Twenty-six positions were chosen and for each position ANSYS would produced numerous results. These results indicated that variation in the mesh stiffness is clearly evident as the gears rotate throughout the meshing cycle. The results here are based on FEA modeling and also on the tooth stiffness change.

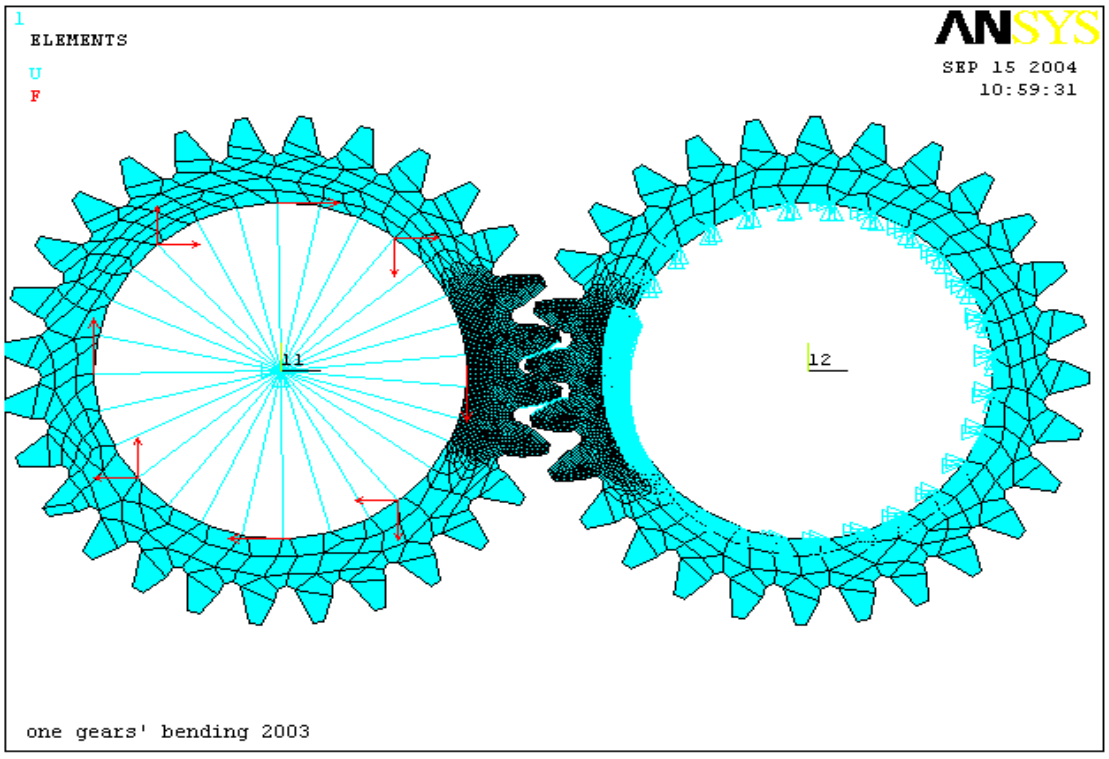


**Figure 5-1 The beam elements were used in the FEA model**

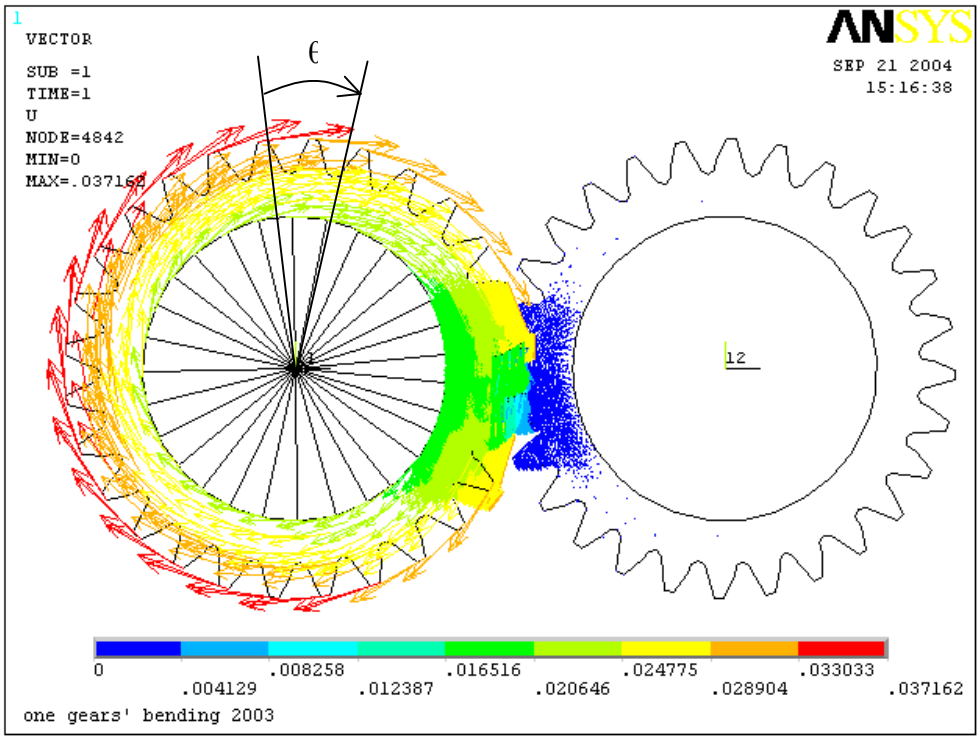


**Figure 5-2 Vectors of displacement**

## 5.3 Transmission Error Model

### 5.3.1 Analysis of the Load Sharing Ratio

Under normal operating conditions, the main source of vibration excitation is from the periodic changes in tooth stiffness due to non-uniform load distributions from the double to single contact zone and then from the single to double contact zone in each meshing cycle of the mating teeth. This indicates that the variation in mesh stiffness can produce considerable vibration and dynamic loading of gears with teeth, in mesh. For the spur involute teeth gears, the load was transmitted between just one to two pairs of teeth gears alternately. The torsional stiffness of two spur gears in mesh varied within the

meshing cycle as the number of teeth in mesh changed from two to one pair of teeth in contact. Usually the torsional stiffness increased as the meshing of the teeth changed

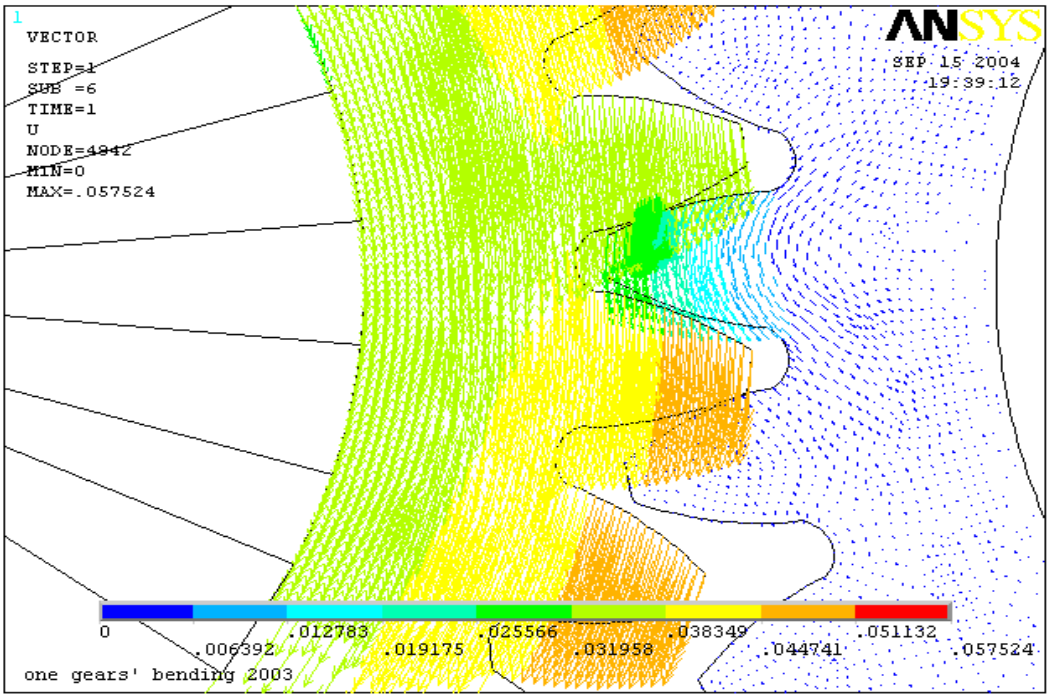


**Figure 5-3 Vectors of displacement near the contact surfaces**

from one pair to two pairs in contact. If the gears were absolutely rigid the tooth load in the zone of the double tooth contacts should be half load of the single tooth contact. However, in reality the teeth become deformed because of the influence of the teeth bending, shear, and contact stresses. These factors change the load distribution along the path of contact. In addition, every gear contains surface finishing and pitching errors. They alter the distribution of load. Because the teeth are comparatively stiff, even small errors may have a large influence. The elastic deformation of a tooth can result in shock loading, which may cause gear failure. In order to prevent shock loading as the gear teeth move into and out of mesh, the tips of the teeth are often modified so as the tooth passes

through the mesh zone the load increases more smoothly. The static transmission error model of gears in mesh can be used to determine the load sharing ratio throughout the mesh cycle. Two identical spur gears in mesh are considered here. Table 5.1 shows the gear parameters.

**Table 5.1 Gear Parameters Used in the Model**

| | |
|---|---|
| Gear Type | Standard Involute, Full-Depth Teeth |
| Modulus of Elasticity, E | 200GPa |
| Module (M) | 3.75 mm |
| Number of Teeth | 27 |
| Pressure Angle | 20 |
| Addendum, Dedendum | 1.00*M, 1.25*M |

### 5.3.2 2D FEA Transmission Error Model

Usually calculation of the static transmission error requires estimation of the loaded teeth deflections. In order to evaluate these required quantities, Tavakoli [61] proposed to model gear teeth using a non uniform cantilever beam. Tobe [62] used a cantilever plate, while numerous authors have developed finite element tooth modeling excluding the contact problem. Unfortunately, the hypotheses related to these models can not be justified because characteristic dimensions of gear teeth are neither representative of a beam nor a plate for the calculation of the static transmission error and tooth deflection behavior changes because of non-linear contact. Most of the previously

published FEA models for gears have involved only a partial tooth model. In this section to investigate the gear transmission error including contact elements, the whole bodies of gears have to be modeled because the penalty of parameter of the contact elements must account for the flexibility of the whole bodies of gears, not just the local stiffness.

Here 2D plane42 elements were used with 2 degrees of freedom per node. The whole model has 5163 nodes, 4751 elements. For the contact surface the contact element was Conta172 and for the target surface the target element was Targe169 shown in Figure 5.4 that matches the position in Figure 5.5. Figure 5.5 displays a meshing model of a spur gear. Fine meshing was used shown in Figure 5.6. The one or two sets of contact elements were enlarged for the single or the double pairs of gears in contact. This operation allows extracting the compliance due to bending and shear deformation, including the contact deformation. This procedure was successively applied to the pinion and the gear.

### 5.3.3 Overcoming the convergence difficulties

In this study the contact stress was always emphasized. The contact problem is usually a challenging problem because contact is a strong nonlinearity. Both the normal and tangential stiffness at the contact surfaces change significantly with changing contact status. Those kinds of large, sudden changes in stiffness often cause severe convergence difficulties. If the constraints established on the model are not proper, it will result zero overall stiffness. In a static analysis unconstrained free bodies are mathematically unstable and the solution “blows up”. In addition, the solution will not be in convergence if the total number of degrees of freedom exceeds 1,000,000.

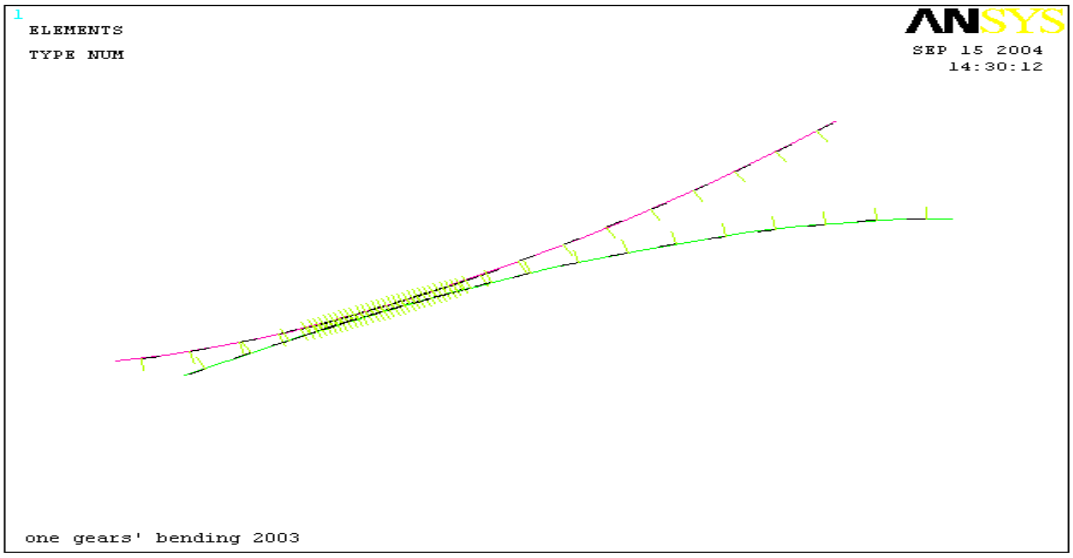


**Figure 5-4 Contact elements between the two contact surfaces**

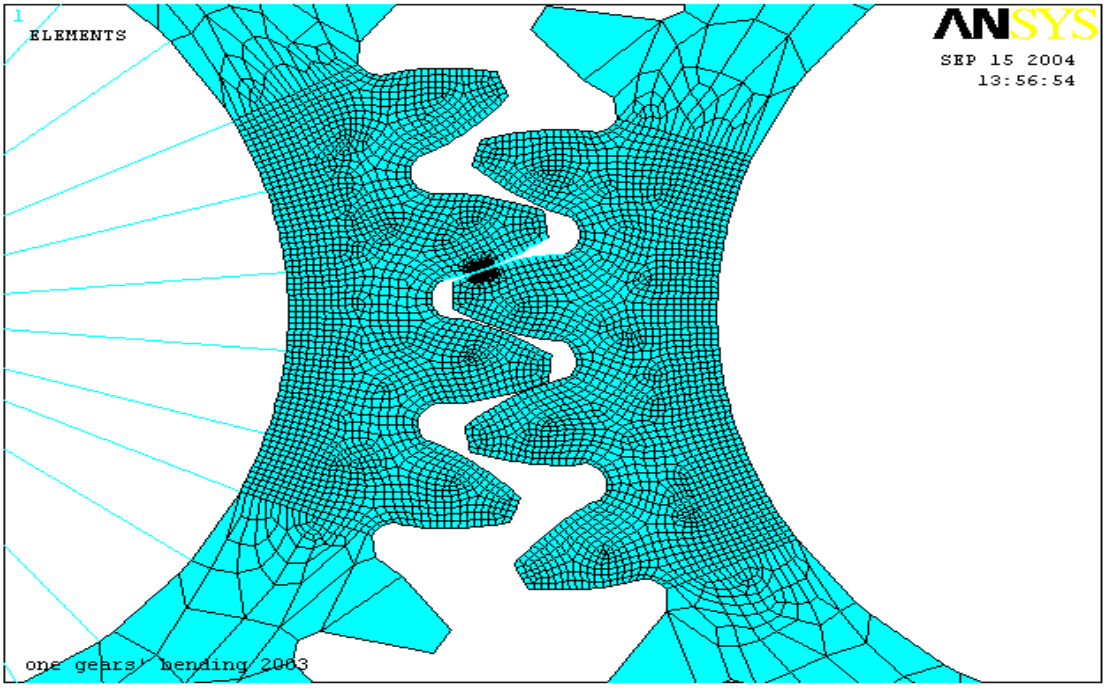


**Figure 5-5 Meshing model for spur gears**

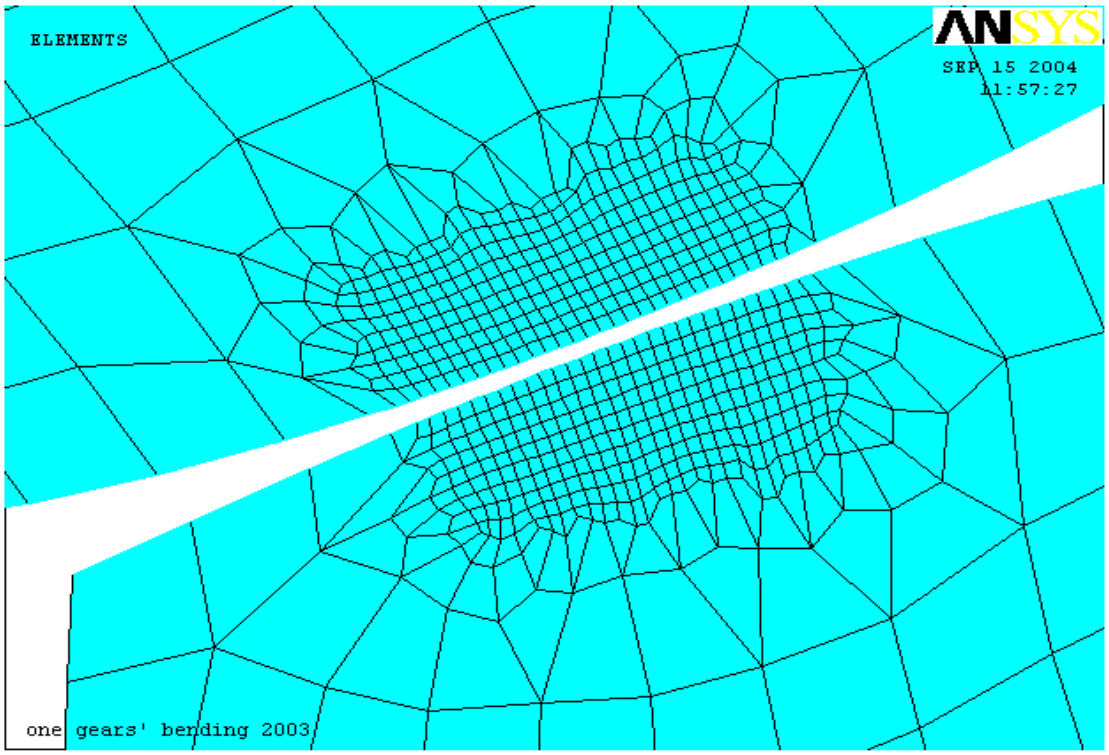


**Figure 5-6 The fine mesh near the two contact surfaces**

The 3D model first exhibited difficult convergence behavior. The output window always displayed: "The system process was out of virtual memory". Or "the value at the certain node is greater than current limit of $10^6$." Several methods were used in order to overcome such difficulties. First, at the beginning a simple model was built. For example, the contact stress between the two square boxes or two circles was obtained using ANSYS. From this simple model, the author learned that it is necessary to make sure there is the enough computer memory for the 3D model so here the 2D model was chosen. It is also very important to allow the certain constraint conditions for the model to be modeled. If the constraints are inadequate, the displacement values at the nodes may

exceed$10^6$. This generally indicates rigid body motion as a result of an unconstrained model so one must verify that the model is properly constrained.

In the author's opinion there are the four important keys to get correct solutions for this FEA model:

Firstly, try to choose the different type of contact element options or choose different element types underlying the contact surfaces. For example, plane42 was chosen instead of the element with middle side nodes on element edges, which make it hard to get convergence. If the elements with middle side nodes were chosen, one must remove the middle side nodes along every element edge before the contact element was built. The total number of the nodes and total number of the elements were thus reduced. This allowed a large amount of computer memory to be saved.

Secondly, there are several choices to deal with the gaps between contact surfaces. For instance, from ANSYS there are three advanced contact features that allow you to adjust the initial contact conditions to prevent the rigid body from moving away:

- Automatic contact adjustment (CNOF) – The program calculates how large the gap is to close the gap,
- Initial contact closure (ICONT) – Moves the nodes on the contact surface within the adjustment band to the target surface,
- Initial allowable penetration range (PMIN & PMAX) – Physically moves the rigid surface into the contact surface.

All three of these methods have been used by trial and error, numerous times. Especially, for the second one, different ICONT values were chosen. ICONT = 0.02, 0.015, 0.012 … However the first one seemed better than other ones. It worked very well.

The first one was chosen for this model. In ANSYS, from Contact Pair in Create from Modeling: Settings > Initial Adjustment > Automatic Contact adjustment: Choose "Close Gap" from listing. Thirdly, if convergence difficulties are encountered, they may generally arise from:

- Too great a value for contact stiffness,
- Too tight a value for penetration tolerance,
- Too large a value for the minimum time step size or too small maximum number of substeps.

So at the beginning in this model the maximum number of substeps is equal to 100. However it took a long time to get convergence. One should try to decrease the number of substeps as long as it can obtain convergence and a certain accuracy. If the maximum number of substeps was equal to 100, it seemed that the accuracy was improved a little but it would take a very long time to solve or to run it. The larger the number of substeps the more time was consumed. This is the reason why the author eventually used 10 as the number of substeps. The normal penalty stiffness is chosen for default. The penetration tolerance is equal to 0.1 (DEFAULT Value). In order to control nonlinear SOLUTION "Large Displacement Static" was chosen from listing. Finally, before going to the solution do not forget the three important things that should be done:

- Merge the node if necessary otherwise it is difficult to get convergence,
- Compress the nodes and the elements to reduce the total number of nodes & elements, and to save more memory in the computer,
- Delete the all the nodes which are not attached the elements.

### 5.3.4 The Results from ANSYS

Here Von Mises stresses and the contact stresses just for one position are shown below in Figure 5.7 and Figure 5.8. For the gears the contact stress was compared with the results from the Hertz equations, and the two results agree with each other well.

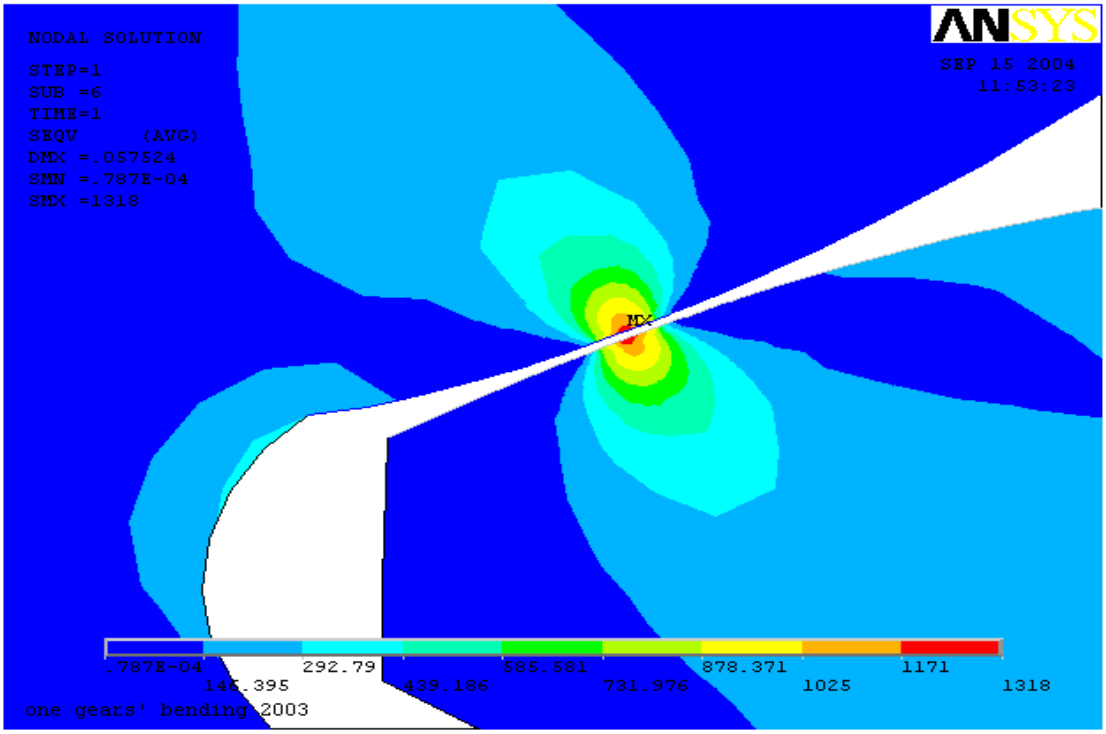


**Figure 5-7 Von Mises stresses in spur gears**

In this model, there are 4751 elements and 5163 nodes. For the contact surfaces there are more than eight nodes on each contact side. So the distribution of contact stresses is resonable. In this chapter the transmission error is emphasized and contact is a nonlinear problem so the solution will likely be done after a greater time compared with the time in linear analysis. It is much simpler to use “WIZARD BAR” and to create contact pair between the contact surfaces from “Preprocessor>Modeling>Create>Contact Pair”.

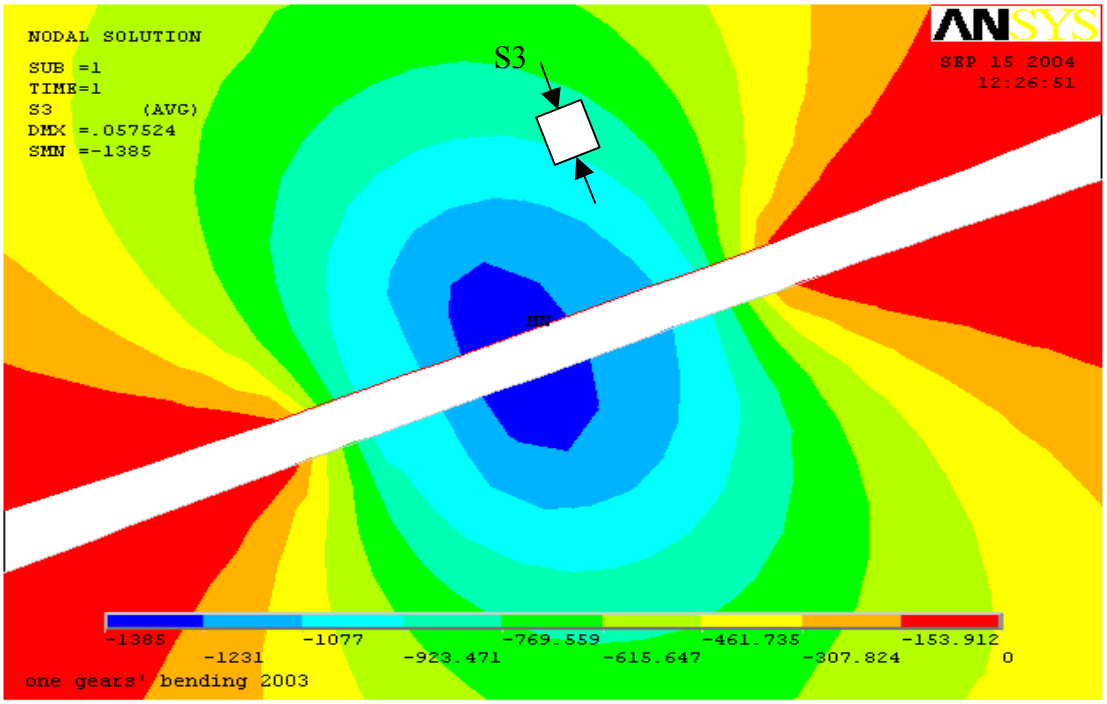


**Figure 5-8 The distribution of contact stresses between two teeth**

## 5.4 The Transmission Error

The static transmission error is expressed as a linear displacement at the pitch point [63]. A kinematic analysis of the gear mesh allows determining the location of contact line for each loaded tooth pair. These contact lines were discretized. The total length of lines of contact grows with the applied load. For each position of the driving gear, the iterative procedures were used to solve the static equilibrium of the gear pair and to calculate the load distribution on the contact lines and the static transmission error. However the contact deformation was excluded in those models.

This section considers a FEA model, which was used to predict static transmission error of a pair of spur gears in mesh including the contact deformation. The

model involves the use of 2-D elements, coupled with contact elements near the points of contact between the meshing teeth. When one pair of teeth is meshing one set of contact elements was established between the two contact surfaces, while when two pairs of teeth are meshing two sets of contact elements were established between the two contact bodies. When gears are unloaded, a pinion and gear with perfect involute profiles should theoretically run with zero transmission error. However, when gears with involute profiles are loaded, the individual torsional mesh stiffness of each gear changes throughout the mesh cycle, causing variations in angular rotation of the gear body and subsequent transmission error. The theoretical changes in the torsional mesh stiffness throughout the mesh cycle match the developed static transmission error using finite element analysis shown in Figure 5.9.

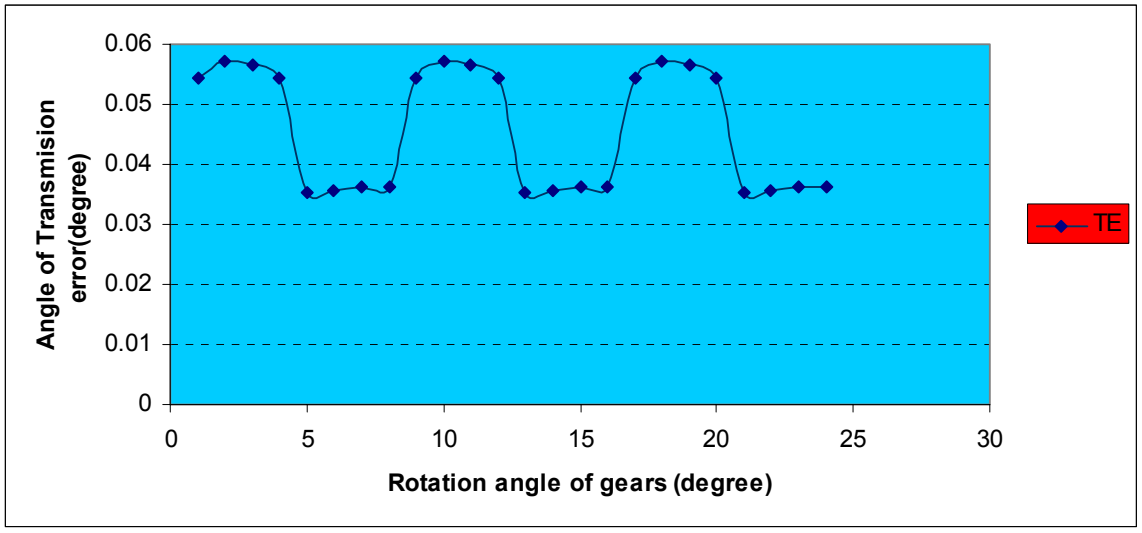


**Figure 5-9 Static transmission error from ANSYS**

## 5.5 Conclusion

Mesh stiffness variation as the number of teeth in contact changes is a primary cause of excitation of gear vibration and noise. This excitation exists even when the gears are perfectly machined and assembled. Numerical methods using 2-D FEM modeling of toothed bodies including contact elements have been developed to analyze the main static transmission error for spur gear pairs. Numerous simulations allowed validating this method and showed that a correct prediction of transmission error needed an accurate modeling of the whole toothed bodies. The elasticity of those bodies modifies the contact between loaded tooth pairs and the transmission error variations. The developed numerical method allows one to optimize the static transmission error characteristics by introducing the suitable tooth modifications. These offer interesting possibilities as first steps of the development of a transmission system and can be also successfully used to improve to control the noise and vibration generated in the transmission system.

# Chapter 6 Conclusions and Future Work

## 6.1 Conclusions

The contribution of the thesis work presented here can be summarized as follows:

It was shown that an FEA model could be used to simulate contact between two bodies accurately by verification of contact stresses between two cylinders in contact and comparison with the Hertzian equations.

Effective methods to estimate the tooth contact stress using a 2D contact stress model and to estimate the root bending stresses using 2D and 3D FEA model are proposed. The analysis of gear contact stress and the investigation of 2D and 3D solid bending stresses are detailed in Chapter 4.

In Chapter 5 the development of a new numerical method for FEA modelling of the whole gear body which can rotate in mesh including the contact problem is presented. The static transmission error was also obtained after running the models in ANSYS.

## 6.2 Future Work

The following areas are worthy of further research as computer capabilities increase. Further numerical method investigations should be conducted on:

- The transmission error for all types of gears for example: helical, spiral bevel and other gear tooth form,
- A whole gearbox with all elements in the system such as the bearing and the gear casing,
- Three-dimensionally meshed simulations for both spur and helical gears,
- Simulation of an oil film in contact zone.

# REFERENCES


[1] Klenz, S. R., 1999, "Finite Element Analyses of A Spur Gear Set", M.Sc. Thesis, Dept. of Mechanical Engineering, University of Saskatchewan.

[2] Umezawa, K., 1988, "Recent Trends in Gearing Technology", JSME International Journal Series III Vol.31, No. 2, pp 357-362

[3] Smith, J. O. Liu, C. K., "Stresses Due to Tangential and Normal Loads on an Elastic Solid with Applications to Some Contact Stress Problems", *Journal of Applied Mechanics*

[4] Norton, R. L., "Machine Design: An Integrated Approach", New Jersey: Prentice-Hall Inc.

[5] Hamrock, B. J., Jacobson, S. R., " Fundamentals of Machine Elements".

[6] Buckingham, E., 1949, "Analytical Mechanics of Gears", McGraw-Hill, New York.

[7] Wang, J., 2003, "Survey of Nonlinear Vibration of Gear Transmission Systems" *Appl Mech Rev* vol 56, No 3.

[8] Chong, T. H., Bar, I., 2001, "Multiobjective optimal Design of Cylindrical Gear Pairs for the Reduction of Gear Size and Meshing Vibration", JSME International Journal, Vol. 44, No. 1, pp 291-292

[9] Coy, J. J., Chao, C. H. S., 1982, "A method of selecting grid size to account for Hertz deformation in finite element analysis of spur gears", Trans. ASME, J. Mech. Design 104 759-766

[10] Gatcombe, E.K., Prowell, R.W., 1960, "Rocket motor gear tooth analysis", (Hertzian contact stresses and times) Trans. ASMA, J. Engng Industry

[11] Tsay, C.B., 1988, "Helical gears with involute shaped teeth: Geometry, computer simulation, tooth contact analysis, and stress analysis", Trans, J. Mechanisms, Transmissions, and Automation in Design

[12] Errichello, R., 1979, “State-of-art review: gear dynamics”, Trans. ASME, J. Mech. Des., 101(3), 368-372.

[13] Ozguven, H. N., Houser. D. R., 1988, “Mathematical models used in gear dynamics”, Sound Vibr., 121,383-411.

[14] Harris, S. L., 1958, “Dynamic load on the teeth of spur gears”, Proc. Instn Meth. Engrs, 172, 87-112.

[15] Mark, W. D., 1978, “Analysis of the vibratory excitation of gear system: Basic theory”, J. Acoust. Soc. Am., 63, 1409-1430.

[16] Mark, W. D., 1979, “Analysis of the vibratory excitation of gear system, II: tooth error representations, approximations, and application”, J. Scouts, Soc. Am., 66, 1758-1787.

[17] Kohler, H., Regan, R., 1985, “The derivation of gear transmission error from pitch error records”, Proc. Instn Mech. Engrs, Part C, Journal of Mechanical Engineering Science, 199(C3), 195-201.

[18] Kubo, A., et al., 1991, “Estimation of transmission error of cylindrical involute gears by tooth contact pattern”, JSME int. J., Ser. III, 34(2), 252-259.

[19] Savage, M., Coy, J.J., 1980, “Optimal Tooth Number for Compact Standard Spur Gear Sets”, by Journal of Mechanical Design, vol.104 749-777

[20] David, L. G., Handschuh F. R., 2001, “Consideration of Moving Tooth Load in Gear Crack Propagation Predictions”, Transations of the ASME vol.123 118-124

[21] Cornell, R. W., Westervelt, W. W., 1978, “Dynamic Tooth Loads and Stressing for High Contact Ratio Spur Gears”, ASME, Journal of Mechanical Design, Jan. Vol. 100

[22] Weber, C., 1949, “The Deformations of Loaded Gears and the Effect on Their Load-Carrying Capacity”, Sponsored Research (Germany), British Dept. of Scientific and Industrial Research, Report No. 3

[23] O’Donnell, W. J., 1974, “Stress and Deflection of Built-in Beams”, ASME Paper No. 62-WA-16

[24] Heywood, R. B., 1952, “Designing by Photoelasticity”, Chapman and Hall, Ltd.

[25] Sweeney, P. J., 1994, “Gear transmission error measurement and analysis”, PhD dissertation, University of New South Wales, Australia

[26] Randall, S. D., Kelly, D.W., “Modeling of spur gear mesh stiffness and static transmission error” , Proc Instn Mech Engrs Vol 212 Part C pp.287-297

[27] Umezawa, K., Sato, T., Ishikawa, J., 1974, “Simulation on Rotational Vibration of spur Gear”, Bull. JSME, Vol. 27, No.223, p.102

[28] Umezawa, K., Suzuki, T., Ishikawa, J., 1987, “On the Design of a Low-Vibration of Helical Gear for Automobiles”, Proc. 4th Int. Pacific Conf. On Automotive Eng., Paper No. 871222

[29] Cockerham, G., 1967, “Computer-Aided Design of Spur or Helical Gear Train”, Computer-Aided Design, Vol.8 No. 2, pp. 84-88.

[30] Tucker,A. I., 1980 “The Gear Design Process”, ASME Paper 80-c2/DET-13

[31] Estrin, M., 1980, “Optimization of Tooth Proportion for a Gear Mesh”, ASME paper 80-C2/DET-101.

[32] Gay, C.E., 1970, “How to Design to Minimize Wear in Gears” , Machine Design, Vol.42, Nov.26, pp.92-97.

[33] Anon., 1966, “Design Procedure for Aircraft Engine and Power Take-Off Spur and Helical Gears”, AGMA Standard No. 411. 02

[34] Howard, I., Jia, S., 2001, “The Dynamic Modeling of Spur Gear in Mesh Including Friction and A Crack”, *Mechanical System and Signal Processing* 15(5), 831-853.

[35] From “www.Google.com”, “Neale Consulting Engineers”, *ncel@tribology.co.uk*

[36] Osman, M., Sankar, S., Dukkipati, R. V., 1978, “Design Synthesis of a Multi-Speed Machine Tool Gear Transmission Using Multiparameter Optimization”, ASME Journal of Mechanical Design, Vol.100, No. 2, pp. 303-310

[37] Kamenatskaya, M. P., 1975, “Computer-Aided Design of Optimal Speed Gearbox Transmission Layouts”, Machines and Tooling, Vol. 46, No.9 pp.11-15

[38] Lim, T. C., 1991, "Vibration Transmission through Rolling Element Bearings, Part III : Geared Rotor System Studies", *Journal of Sound and Vibration*,153(1), pp 31-54.

[39] Andersson, S. A. E., 1973, "On the design of internal Involute Spur Gears", Transactions of Machine Elements Division, Lund Technical University, Lund, Sweden.

[40] Anon, 1966, "Rating the Strength of Spur Teeth", AGMA Standard 220.02.

[41] Kahraman, A., 1992, "Dynamic Analysis of Geared Rotors by Finite Elements", *Journal of Mechanical Design,* 114 (September), pp 507-514.

[42] Ishikawa, H., 1989, "An Effective Method for Three-Dimensional Finite Element Analysis of a Gear Pair under Partial Contact", JSME International Journal Series III Vol.32, No. 2, pp 246-252

[43] Anon., 1965, "Surface Durability (Pitting) of Spur Teeth", AGMA Standard 210.02.

[44] Coy, J.J., Townsend, D.P., Zaresky,E. V., 1976, "Dynamic Capacity and Surface Fatigue Life for Spur and Helical Gears", ASMA Journal of Lubrication Technology, Vol.98, No. 2, Pre. pp.267-276.

[45] Bowen, C. W., 1978, "The Practical Significance of Designing to Gear Pitting Fatigue Life Criteria", ASMA Journal of Mechanical Design, Vol.100, No. 1 pp.46-53.

[46] Anon., 1965, "Gear Scoring Design Guide for Aerospace Spur and Helical Power Gear", AGMA Information Sheet 217.01.

[47] Rozeanu, L., Godet, M., 1977, "Model for Gear Scoring" ,ASME Paper 77-DET-60.

[48] Kasuba R., Evans, J. W. 1981, "An Extended Model for Determining Dynamic Loads in Spur Gearing"

[49] Stadler, W., Dauer, J., 1992, " Multicriteria Optimization in Engineering: A Tutorial and Survey", Structural Optimization: Status and Promise, Progress in Aeronautics, Edited by M. P. Kamat,150,pp.209-244

[50] Hwang, C.L., Masud, A. S. M., 1979, "Multiple Objective Decision Making-Methods and Applications, Springer-Verlag,Berlin"

[51] Tappeta, R. V., Renaud, J. E., 1999, "Interative MultiObjective Optimization Procedure", AIAA J.,37, No,7, July,pp881-889

[52] Tappeta, R. V., 2001, "Interactive Multiobjective Optimization Design Strategy for Decision Based Design", Journal of Mechanical Design. Vol, 123 pp.205-215.

[53] Nicoletto, G., 1993, "Approximate Stress Intensity Factors for Cracked Gear Teeth", Eng. Fract. Mech., 44. No.2, pp. 231-242

[54] Sfakiotakis, V. G., Katsareas, D.E., Anifantis, N. K., 1997, "Boundary Element Analysis of Gear Teeth Fracture", Eng. Anal Boundary Elem., 20, No. 2, pp. 169-175

[55] Blarasin, A., Guagliano, M., Vergani, L., 1997, "Fatigue Crack Growth Predictions in Specimens Similar to Spur Gear Teeth", Fatigue Fract. Eng. Mater. Struct., 20, No. 8,pp. 1171-1182.

[56] Lewicki, D.G., Ballarini, R., 1997, "Experimental Analysis of Propagation of Fatigue Crack on Gears", Exp. Mech., 38, No. 3, pp. 226-230.

[57] Perret-Liaudet, J., Sabot, J., 1994, "Dynamics of Truck Gearbox", 6th International Power Transmission and Gearing Conference, Scottdale, Arizona, USA, pp 249-258.

[58] Vijayarangan S., Ganesan N. 1994, "Static Contact Stress Analysis of A Spur Gear Tooth Using the Finite Element Method Including Friction Effects", Computer & Struture Vol. 51 No. 6 pp767-770

[59] Smith, J. D. 1983, "Gears and Their Vibration", Marcel Dekker, New York

[60] Sirichai, S. et al 1997, "Finite Element Analysis of gears in Mesh", Fifth International Congress on Sound and Vibration, Australia, pp 869-876.

[61] Tavakoli M., Houser D., 1986, "Optimum Profile Modifications for the minimization of Static Transmission Errors of Spur Gears", Journal of Mechanisms, Transmission and Automation in Design, Vol. 108, pp 86-95.

[62] Tobe T., Kato, M., Inoue K., 1978, "Bending of Stub Cantilever Plate and some Application to Strength of Gear Teeth", Journal of Mechanical Design, Vol. 100, pp 374-381.

[63] Rigaud, E. “Modelling and Analysis of Static Transmission Error – Effect of Wheel Body Deformation and Interactions Between Adjacent Loaded Teeth”

[64] Sirichai S., 1999, “Torsional Properties of Spur Gear in Mesh using nonlinear Finite Element Analysis”, Ph.D. Thesis, Curtin University of Technology.

[65] B.J. Hamrock, B. Jacobson, S. R. Schmid 1999, “Fundamentals of Machine Elements”

[66] Kasuba, R., “An Analytical and experimental Study of dynamic Loads on Spur Gear Teeth”, Ph.D., University of Illinolis

[67] Aida, T., 1969, “Fundamental Research on Gear Noise and Vibration I”, *Transaction of the Japanese Society of Mechanical Engineering,* 35, pp. 2113-2119

[68] Tordian, G. V., 1967, “dynamic Measurement of the Transmission Error in Gear”, *Proc. JSME Semi-International Symposium September* , pp. 279-287

# Appendix A Input File of A Model of Two Cylinders

```
!*********************************************
!           Parameter Definitions
!*********************************************
!Cyclinder Geometry and Materials
*SET,PI,acos(-1)
*SET,F,91.545
*SET,R1,3
*SET,R2,3
*SET,v1,0.3
*SET,v2,0.3
*SET,E1,30e6
*SET,E2,30e6
*SET,L,1
*SET,ptype,2
!Loading Controls
*SET,st1,1
*SET,st2,1
*SET,st3,1
*SET,st4,1
*SET,kn,10e8
*SET,coloumb,1
*SET,mu,0.1
*SET,tol,1e-6
!Load Step Options
*SET,disp,-1e-6
*SET,pnot,0.20
*SET,ns2i,5
*SET,ns3i,5
*SET,ns4i,4
```

```
*SET,rotate1,0
*SET,rotate2,0
*SET,rot,0*2
!Model Size
*SET,hi,0.5
*SET,wi,1.4
!Meshing Controls
*SET,elemtype,1
*SET,nec,10
*SET,ratio1,50
*SET,ratio2,25
!Non-Contact Element Properties
*SET,etop,30e9
*SET,itop,355
*SET,atop,555
!Calculated Values
*SET,delta,(1-v1**2)/E1+(1-v2**2)/E2
*SET,po,0.564*(F*(1/R1+1/R2)/(L*delta))**0.5
*SET,b,1.13*(F*delta/(1*(1/R1+1/R2)))**0.5
!*SET,b,1.08*sqrt(F*R1/E1)
*SET,dx,2*b/nec
*SET,gamma1,atan(b/R1)
*SET,gamma2,atan(b/R2)
/title, Two cylinders' contact 2002 with friction
!*************************************************
!               Geometry Generation
!*************************************************
/prep7
*SET,delta,gamma1/nec*180/pi*rot
local,11,1,0,R1+R2+1e-9,,delta
csys,1
/pnum,line,1
```

```
/pnum,kp,1
k,1
k,2,R1+R2+1e-9,90
k,3,R2,180
k,4,R2,90+gamma2*wi*180/pi
k,5,R2-hi*2*b,90+gamma2*wi*180/pi
k,6,R2-hi*2*b,90-gamma2*wi*180/pi
k,7,R2,90-gamma2*wi*180/pi
k,8,R2,0
k,15,R2/2,180
k,16,R2/2,0
k,19,R2-hi*2*b,90
k,21,R2,90+100*gamma2*wi*180/pi
k,22,R2-hi*100*b,90+100*gamma2*wi*160/pi
k,23,R2-hi*180*b,90
k,24,R2-hi*100*b,90-100*gamma2*wi*160/pi
k,25,R2,90-100*gamma2*wi*180/pi
larc,3,21,1,R2
larc,21,4,1,R2
l,4,5
l,5,19
l,19,6
l,6,7
larc,7,4,1,R2
larc,7,25,1,R2
larc,25,8,1,R2
l,8,16
l,16,1
l,1,15
l,15,3
l,6,24
l,24,16
```

l,5,22
l,22,15
l,19,23
l,23,1
l,21,22
l,22,23
l,23,24
l,24,25
csys,11
k,9,R1
k,10,R1,-90+gamma1*wi*180/pi
k,11,R1-hi*2*b,-90+gamma1*wi*180/pi
k,12,R1-hi*2*b,-90-gamma1*wi*180/pi
k,13,R1,-90-gamma1*wi*180/pi
k,14,R1,-180
k,17,R1/2
k,18,R1/2,-180
k,20,R1-hi*2*b,-90
k,26,R1,-90-100*gamma1*wi*180/pi
k,27,R1-hi*100*b,-90-100*gamma1*wi*160/pi
k,28,R1-hi*180*b,-90
k,29,R1-hi*100*b,-90+100*gamma1*wi*160/pi
k,30,R1,-90+100*gamma1*wi*180/pi
larc,14,26,2,R1
larc,26,13,2,R1
larc,13,10,2,R1
l,10,11
l,11,20
l,20,12
l,12,13
larc,10,30,2,R1
larc,30,9,2,R1

l,9,17
l,17,2
l,2,18
l,18,14
l,11,29
l,29,17
l,12,27
l,27,18
l,20,28
l,28,2
l,26,27
l,27,28
l,28,29
l,29,30
al,3,4,5,6,7
al,26,27,28,29,30
al,2,20,16,3
al,1,13,17,20
al,16,21,18,4
al,17,12,19,21
al,18,22,14,5
al,19,11,15,22
al,6,14,23,8
al,15,10,9,23
al,25,30,39,43
al,39,29,41,44
al,41,28,37,45
al,37,27,31,46
al,24,43,40,36
al,40,44,42,35
al,42,45,38,34
al,38,46,32,33

```
!*****************************************************
!                    Meshing
!*****************************************************
!Define element type
*if,elemtype,eq,1,then
et,1,plane42,,,ptype
*else
et,1,plane82,,,ptype
*endif
mp,ex,1,30e6
mp,nuxy,1,0.3
eshape,3
real,1
mat,1
type,1
lesize,3,dx
lesize,4,dx
lesize,5,dx
lesize,6,dx
lesize,7,dx
lesize,26,dx
lesize,27,dx
lesize,28,dx
lesize,29,dx
lesize,30,dx
asel,all
amesh,all
*if,elemtype,eq,2,then
modmesh,detach
type,1
csys,1
nsel,s,loc,x,r2-1e-4,r2+1e-10
```

```
esln,s,0
emid,remove,both
csys,11
nsel,s,loc,x,r1-1e-4,r1+1e-10
esln,s,0
emid,remove,both
allsel
nsel,all
nsel,inve
ndele,all
allsel
*endif
!Define and Generate contact elements
et,2,contac48,,0,coloumb,,,,1
r,2,kn,kn,,1,tol
mp,mu,2,mu
type,2
real,2
mat,2
!Generate contact elements on one surface
csys,11
nsel,s,loc,x,r1-1e-10,r1+1e-10
nsel,r,loc,y,-90-3*gamma1*180/pi,-90+3*gamma1*180/pi
cm,uppern,node
!Generate contact elements on the other surface
csys,1
nsel,s,loc,x,r2-1e-10,r2+1e-10
nsel,r,loc,y,90-3*gamma2*180/pi,90+3*gamma2*180/pi
cm,lowern,node
csys,0
gcgen,uppern,lowern
gcgen,lowern,uppern
```

```
allsel
!Generate .....
n,,0,r1+r2+1e-9
nsel,s,loc,x,0-1e-8,0+1e-8
nsel,r,loc,y,r1+r2,r1+r2+2e-9
*get,ntop,node,,num,max
nsel,all
csys,11
nsel,s,loc,x,R1-1e-12,R1+1e-12
nsel,r,loc,y,-180-1e-12,-180+1e-12
*get,natkp14,node,,num,max
nsel,all
nsel,s,loc,x,R1-1e-12,R1+1e-12
nsel,r,loc,y,0-1e-12,0+1e-12
*get,natkp9,node,,num,max
nsel,all
et,4,beam3
r,4,atop,itop,1
mp,ex,4,etop
mp,nuxy,4,0.3
mat,4
type,4
real,4
lmesh,33
lmesh,34
lmesh,35
lmesh,36
nsel,all
e,ntop,natkp14
e,ntop,natkp9
!*****************************************************
!               Boundary Conditions
```

```
!*************************************************

!Rotate all nodes in upper cylinder to be in a cylindrical system
csys,0
allsel
nsel,s,loc,y,R2+1e-12,400
cm,upper,node
allsel
csys,11
nrotate,all
csys,0
nsel,s,loc,y,0,R2+1e-10
cm,lower,node
csys,1
nrotate,all
!Fix bottom of lower cylinder
csys,0
nsel,s,loc,x,-R2,R2
nsel,r,loc,y,0
d,all,all
!Eliminate lateral motion of upper cylinder's totation center
nsel,s,node,,ntop
csys,0
nrotate,all
d,ntop,ux,0
allsel
wsort
/dist,,dist
/focus,,0,center
/pbc,u,1
/pbc,f,1
/dscale,all,1
```

```
eplot
!*************************************************************
!                    Solution
!*************************************************************
/solu
load=F
!***********Load Step 1 ***********
*if,st1,eq,1,then
d,ntop,uy,disp
d,ntop,rotz,0
neqit,25
allsel
solve
*endif
!***********Load Step 2************
*If,st2,eq,1,then
ddele,ntop,uy
ddele,ntop,rotz
d,ntop,rotz,rotate1
!Apply a pressure
csys,0
nsel,s,loc,x,0
nsel,r,loc,y,R1+R1
f,all,fy,-load*pnot
csys,0
nsubst,ns2i,,1
neqit,200
allsel
solve
save
*endif
```

```
!**********Load Step 3**********
*if,st3,eq,1,then
ddele,ntop,rotz
nsubst,ns3i,,1
csys,0
nsel,s,loc,x,0
nsel,r,loc,y,R1+R2
f,all,fy,-load
/psf,pres,2
csys,0
allsel
solve
*endif

!**********Load Step 4**********
*if,1,eq,st4,then
d,ntop,rotz,-5e-3
csys,0
nsubst,ns4i,,1
neqit,10
allsel
solve
*endif
finish
```